CDF/ANAL/HEAVYFLAVOR/CDFR/1930

DRAFT Version 1.0

A Measurement of the Correlated $b\bar{b}$ Cross Section

R. Mattingly, P. Sphicas

Abstract

We describe a measurement of the cross section for the production of $b\bar{b}$ pairs using data taken during the 1988-1989 Fermilab collider run. We use high mass $e\mu$ events to determine $\sigma(p\bar{p} \rightarrow b_1 b_2 X : P_{T,1} > P_{T,1}^{min}, \mid y_1 \mid < 1; P_{T,2} > P_{T,2}^{min}, \mid y_2 \mid < 1; M_{e\mu} > 5)$ for three pairs of $(P_{T,1}^{min}, P_{T,2}^{min})$ values. We also extract the single-b inclusive cross section, $\sigma(p\bar{p} \rightarrow bX : P_T^b > 8.75 \text{ GeV}, \mid y^b \mid < 1)$, using the correlated cross section and the MNR Monte Carlo.

1 Introduction and Overview

The purpose of this note is to describe the measurement of the cross section for correlated bottom quark production using high mass $e\mu$ pairs. This note is organized as follows:

1.0 Introduction and Overview

1.1 The Correlated $b\bar{b}$ Cross Section

1.2 Tagging $b\bar{b}$

1.3 Sources of $e\mu$ pairs

1.4 The Method for Measuring $\sigma(b\bar{b}\ X)$

2.0 The $e\mu$ Data Set

2.1 The Analysis Data Set

2.2 The Unbiased Data Set

3.0 The Lepton Quality Cuts and the Determination of R_Δ

4.0 The Trigger Efficiency

5.0 The Electron and Muon Acceptances

6.0 Determining $f_{b\bar{b}}$

7.0 $\sigma(b\bar{b}\ X)$

1.1 The Correlated $b\bar{b}$ Cross Section

We first shall attempt to describe in some detail exactly what is meant by the 'correlated' cross section so as to avoid any possible confusion. Previous measurments of cross sections for bottom quark production at hadron colliders have all quoted values for the observation of a single quark above a certain P_T and within a certain interval in rapidity ,*i.e.* $\sigma(p\bar{p} \rightarrow bX; P_{T,b} > P_T^{min}, \mid y_b \mid < y_{max})$. The correlated measurement is the cross section for the observation of two bottom quarks in an event where each quark has a P_T above a certain threshold and has a rapidity within a certain range; such a measurement may be written symbolically as $\sigma(p\bar{p} \rightarrow b_1 b_2 X; P_{T,1} > P_{T,1}^{min}, \mid y_1 \mid < y_{max,1}; P_{T,2} > P_{T,2}^{min}, \mid y_2 \mid < y_{max,2})$. These two cross sections differ in that one is sensitive to the kinematics of a single quark only and the other is sensitive to the kinematics

of both quarks in an event. Because of the sensitivity to both quarks, the measurement is dependent upon kinematical correlations between those two quarks. One may alternately refer to $\sigma(p\bar{p} \rightarrow bX; ...)$ as the single-inclusive cross section and to $\sigma(p\bar{p} \rightarrow b\bar{b}X; ...)$ as the double-inclusive cross section.

1.2 Tagging $b\bar{b}$

A measurement of a bottom quark cross section first requires a method for tagging bottom quarks. The added challenge of this analysis is that a method is required for identifying both quarks in an event. An obvious first choice would have been to tag one b via a decay such as $J/\psi K$ and to then use a semileptonic decay to tag the other quark. This strategy leads to a rate which is too low to be of practical use. The J/ψ sample contains only a handfull of events for which there is a third, good lepton. We chose to look for events where both bottom quarks decayed semileptonically in order to obtain a high enough rate for a reasonable measurement. More specifically, we chose to look for events in which one b decayed to an electron and the other to a muon, thus avoiding potential backgrounds such as Drell Yan, and leptonic decays of the J/ψ, Υ, and Z.

1.3 Sources of Electron-Muon Pairs

Having chosen the $b\bar{b} \rightarrow e\mu X$ decay mode, we must consider the sources of events with electron-muon pairs and the characteristics of those events.

The events of greatest interest are, of course, those in which the lepton pair comes from the decay of a pair of bottom quarks. The lepton may come directly from the b or indirectly from the b through the decay of the daughter charm quark.

$$b \rightarrow \ell c\nu \quad \text{Direct lepton}$$

$$b \rightarrow cX, c \rightarrow \ell X \quad \text{Indirect lepton}$$

In the absence of $b\bar{b}$ mixing, two direct leptons would always have opposite charges

$$b \rightarrow \ell^- X,\ \bar{b} \rightarrow \ell^+ Y$$

whereas one direct and one indirect would have the same sign charges

$$b \to \ell^- X,\ \bar{b} \to \bar{c}Y \to \ell^- Y$$

and two indirect leptons would have opposite sign charges

$$b \to cX \to \ell^+ X,\ \bar{b} \to \bar{c}Y \to \ell^- Y$$

Bottom quarks do undergo mixing and this modifies the situation somewhat. We use the usual parameter, χ, which describes the probablility that a bottom quark will undergo mixing

$$\chi \equiv \frac{Prob(b \to \overline{B^0} \to B^0 \to \ell^+)}{Prob(b \to \overline{B} \to \ell^\pm)}$$

where B^0 refers to either B_d^0 or B_s^0 and B represents any bottom flavored hadron. We may then write, in terms of χ, what the probabilites are that: neither of the bottom quarks mix

$$Prob(\text{neither mix}) = (1-\chi)^2$$

that both the quarks mix

$$Prob(\text{both mix}) = \chi^2$$

and that only one of the quarks mixes

$$Prob(\text{one mixes}) = 2\chi(1-\chi)$$

where the factor of two is due to there being two quarks that can mix. Defining $P_{b\ell}$ as the probability of observing a direct lepton from a bottom decay and $P_{bc\ell}$ as the probability of observing an indirect lepton, the probabilities of a $b\bar{b}$ pair yielding an opposite sign (os) $e\mu$ pair or a same sign (ss) pair are respectively:

$$\begin{aligned} Prob(b\bar{b} \to e\mu; os) &= (2P_{be}P_{b\mu} + 2P_{bce}P_{bc\mu})(Prob(\text{neither mix}) + Prob(\text{both mix})) \\ &+ (2P_{be}P_{bc\mu} + 2P_{bce}P_{b\mu})Prob(\text{one mixes}) \\ &= (2P_{be}P_{b\mu} + 2P_{bce}P_{bc\mu})((1-\chi)^2 + \chi^2) + (2P_{be}P_{bc\mu} + 2P_{bce}P_{b\mu})2\chi(1-\chi) \end{aligned}$$

$$Prob(b\bar{b} \to e\mu; ss) = (2P_{be}P_{b\mu} + 2P_{bce}P_{bc\mu})Prob(\text{one mixes})$$

$$+ \quad (2P_{be}P_{bc\mu} + 2P_{bce}P_{b\mu})(Prob(\text{neither mix}) + Prob(\text{both mix}))$$

$$= \quad (2P_{be}P_{b\mu} + 2P_{bce}P_{bc\mu})2\chi(1-\chi) + (2P_{be}P_{bc\mu} + 2P_{bce}P_{b\mu})((1-\chi)^2 + \chi^2)$$

The difference in the probabilities is

$$\begin{aligned} Prob(os) - Prob(ss) &= Prob(b\bar{b} \rightarrow e\mu; os) - Prob(b\bar{b} \rightarrow e\mu; ss) \\ &= (1-2\chi)^2 2(P_{be}P_{b\mu} + P_{bce}P_{bc\mu} - P_{be}P_{bc\mu} - P_{bce}P_{b\mu}) \\ &= (1-2\chi)^2 2(P) \end{aligned}$$

An electron-muon pair may also come from the cascade decay of a single bottom quark.

$$b \rightarrow \ell^- c\nu, \; c \rightarrow \ell^+ s\nu$$

Such pairs are always of opposite sign. They are easily removed from a data set by demanding that the $e\mu$ invariant mass be greater than the mass of the b.

The dual semileptonic decay of a pair of directly produced charm quarks can also lead to an electron and a muon in the final state.

$$p\bar{p} \rightarrow c\bar{c} \rightarrow e\mu X$$

As there is negligible mixing, the leptons will always be of opposite sign. The contribution from $c\bar{c}$ is expected to be small relative to that from $b\bar{b}$ as the P_T spectrum of leptons from $c\bar{c}$ is much softer than that for leptons from $b\bar{b}$.

Events may also be composed of electrons or muons that are of non-prompt origin or are, in reality, misidentified particles. Example of leptons from non-prompt sources are electrons from photon conversions and muons from decays-in-flight. Muon and electron signatures in the detector may be produced by other particles or combinations of other particles. A particle which does not shower in the calorimetry may reach the muon chambers and be misidentified as a muon. Overlapping π^0s and charged pions may be midientified as an electron. Non-prompt or misidentified particles will be referred to as 'fakes' and events in which one or both of the leptons are fake will be referred to as fake events. Since the processes which produce fake electrons and muons are random with respect to the charge of the fake produced, fake events are equally likely to have $e\mu$ pairs of opposite sign or of same sign.

1.4 The Method for Measuring $\sigma(b\bar{b}\ X)$

The correlated cross section may be written in the usual way

$$\begin{aligned}\sigma(p\bar{p} \rightarrow b\bar{b}\ X) &\equiv \sigma(p\bar{p} \rightarrow b_1 b_2 X; P_{T,1} > P_{T,1}^{min}, \mid y_1 \mid < y_{max,1}; P_{T,2} > P_{T,2}^{min}, \mid y_2 \mid < y_{max,2}) \\ &= \frac{N_{b\bar{b}}^{cre}(P_{T,1} > P_{T,1}^{min}, \mid y_1 \mid < y_{max,1}; P_{T,2} > P_{T,2}^{min}, \mid y_2 \mid < y_{max,2})}{\mathcal{L}}\end{aligned}$$

where $N_{b\bar{b}}^{cre}$ is the number of $b\bar{b}$ pairs produced within the given kinematical constraints for a certain integrated luminosity, $\mathcal{L}$. We must relate $N_{b\bar{b}}^{cre}$ to the data. The number of electron-muon events after all cuts may be written as

$$N_{e\mu} = N_{b\bar{b}} + N_{c\bar{c}} + F$$

$N_{b\bar{b}}$ and $N_{c\bar{c}}$ represent the number of events due to $b\bar{b}$ and $c\bar{c}$ respectively, and F the number of fake events. Splitting the events into *os* and *ss* contributions

$$N_{e\mu}^{os} = N_{b\bar{b}}^{os} + N_{c\bar{c}} + \frac{1}{2}F$$

$$N_{e\mu}^{ss} = N_{b\bar{b}}^{ss} + \frac{1}{2}F$$

we note that the fake contribution may be subtracted out

$$\Delta_{e\mu} = N_{e\mu}^{os} - N_{e\mu}^{ss} = N_{b\bar{b}}^{os} - N_{b\bar{b}}^{ss} + N_{c\bar{c}} = \Delta_{b\bar{b}} + N_{c\bar{c}}$$

The subtraction of the *os* and *ss* $e\mu$ pairs removes, within the limits of statistical uncertainty, the contribution from events in which one or both of the leptons is a fake. The events remaining after the subtracion are due to $b\bar{b}$ and $c\bar{c}$ production. The $b\bar{b}$ contribution includes events in which both leptons come directly from the b decay, events in which one lepton comes directly from the b and one comes indirectly from a b via a sequential charm decay, and events in which both leptons come indirectly from b's via sequential charm decays. We may explicitly indicate the fraction of the sign-subtracted $e\mu$ events due to $b\bar{b}$ production and $c\bar{c}$ production:

$$\Delta_{e\mu} = (f_{b\bar{b}} + f_{c\bar{c}})\Delta_{e\mu}$$

$$f_{b\bar{b}} \equiv \frac{\Delta_{b\bar{b}}}{\Delta_{e\mu}},\ f_{c\bar{c}} \equiv \frac{N_{c\bar{c}}}{\Delta_{e\mu}}$$

The number of $b\bar{b}$ events remaining after sign-subtraction, Δ_{bb}, may be expressed in terms of N_{bb}^{cre} and the previously discussed probabilities for observing an *os* or *ss* $e\mu$ pair.

$$\Delta_{bb} = N_{bb}^{os} - N_{bb}^{ss} = (Prob(os) - Prob(ss))N_{bb}^{cre}$$

It follows that:

$$f_{bb}\Delta_{e\mu} = \Delta_{bb} = (1-2\chi)^2 2(P) N_{bb}^{cre}$$

$$N_{bb}^{cre} = \frac{f_{bb}\Delta_{e\mu}}{(1-2\chi)^2 2(P)}$$

We now have a relation between the number of $b\bar{b}$ pairs created and the number of sign-subtracted $e\mu$ events observed in the data; dividing by the integrated luminosity yields the following expression for the cross section:

$$\sigma(p\bar{p} \rightarrow b\bar{b}\, X) = \frac{f_{bb}\Delta_{e\mu}}{\mathcal{L}(1-2\chi)^2 2(P)}$$

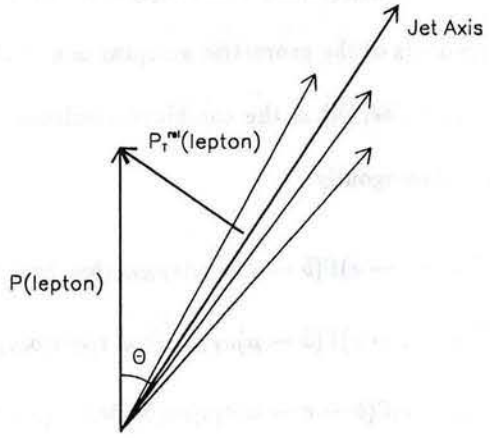

Figure 1: An illustration of the definition of P_T^{rel}.

The fraction of the events due to $b\bar{b}$ production remaining in our sample after the imposition of all cuts is represented by f_{bb}; this quantity can be determined from the data by examination of the P_T^{rel} distributions for the electron and muon. P_T^{rel} is defined as the transverse momentum of the lepton relative to the axis of an associated jet; this quantity is illustrated in Figure 1. P_T^{rel} is, in a sense, a measure of the invariant mass

the decaying particle; hence, the distribution of P_T^{rel} is different for bs and cs . The angle between the lepton and the hadronic remnants in a b decay will be larger than that for c decay because of the greater invariant mass of the bottom quark; hence, the P_T^{rel} distribution for bs will be stiffer that that for cs. The P_T^{rel} distribution for the $e\mu$ data can be produced for the os and ss pairs and the difference of the distributions fitted with the sum of the appropriate bottom and charm distributions to obtain the $b\bar{b}$ fraction. The $b\bar{b}$ fraction is expected to be close to 100% because of the relative softness of leptons from $c\bar{c}$ compared to $b\bar{b}$.

The factor, $(1-2\chi)^2 2(P)$, represents the difference in the probabilities for observing an oppositely signed $e\mu$ pair due to $b\bar{b}$ production and a same signed $e\mu$ pair due to $b\bar{b}$ production.

$$(P) = P_{be}P_{b\mu} + P_{bce}P_{bc\mu} - P_{be}P_{bc\mu} - P_{bce}P_{b\mu}$$

Recalling that $P_{b\ell}$ is the probability of observing a direct lepton from a b decay and $P_{bc\ell}$ the probability of observing an indirect lepton from a b decay ($\ell = e, \mu$), we write

$$P_{be}P_{b\mu} = \Gamma(b \to e)\Gamma(b \to \mu)\epsilon_{TRIG}(be, b\mu)A(be)A(b\mu)\epsilon_{CUTS}(be, b\mu)$$

The Γs are branching fractions. $\epsilon_{TRIG}(be, b\mu)$ is the trigger efficiency for a direct electron and a direct muon. $A(be)$ and $A(b\mu)$ are the products of the geometric acceptance and the acceptance in P_T for direct electrons and muons, respectively. $\epsilon_{CUTS}(be, b\mu)$ is the combined efficiency of all the cuts for events with a direct electron and a direct muon. Analogously:

$$\begin{aligned}
P_{bce}P_{bc\mu} &= \Gamma(b \to c \to e)\Gamma(b \to c \to \mu)\epsilon_{TRIG}(bce, bc\mu)A(bce)A(bc\mu)\epsilon_{CUTS}(bce, bc\mu) \\
P_{bce}P_{b\mu} &= \Gamma(b \to c \to e)\Gamma(b \to \mu)\epsilon_{TRIG}(bce, b\mu)A(bce)A(b\mu)\epsilon_{CUTS}(bce, b\mu) \\
P_{be}P_{bc\mu} &= \Gamma(b \to e)\Gamma(b \to c \to \mu)\epsilon_{TRIG}(be, bc\mu)A(be)A(bc\mu)\epsilon_{CUTS}(be, bc\mu)
\end{aligned}$$

We may define a quantity, (p), similar to (P) such that

$$(p) = p_{be}p_{b\mu} + p_{bce}p_{bc\mu} - p_{be}p_{bc\mu} - p_{bce}p_{b\mu}$$

where,

$$p_{be}p_{b\mu} = \frac{1}{\epsilon_{CUTS}(be, b\mu)}P_{be}P_{b\mu} = \Gamma(b \to e)\Gamma(b \to \mu)\epsilon_{TRIG}(be, b\mu)A(be)A(b\mu)$$

with $p_{bce}p_{bc\mu}$, etc. defined analogously. The factor, $(1-2\chi)^2 2(P)$, is the difference in the probabilities for observing *os* and *ss* $e\mu$ pairs due to $b\bar{b}$ production after the imposition of all cuts, whereas the factor, $(1-2\chi)^2 2(p)$, is the difference in the probalilities for observing *os* and *ss* $e\mu$ pairs due to $b\bar{b}$ production prior to the imposition of any cuts. We have previously defined $\Delta_{e\mu}$ as the number of sign-subtracted $e\mu$ events after the imposition of all cuts. The number of sign-subtracted $e\mu$ events prior to the imposition of any cuts is denoted by $\Delta_{e\mu}^{raw}$. These two quantities may be written in terms of the number of $b\bar{b}$ pairs created, $N_{b\bar{b}}^{cre}$, χ, (P), and (p).

$$\begin{aligned} \Delta_{e\mu} &= (1-2\chi)^2 2(P) N_{b\bar{b}}^{cre} \\ \Delta_{e\mu}^{raw} &= (1-2\chi)^2 2(p) N_{b\bar{b}}^{cre} \end{aligned}$$

In general, the above expressions should include terms describing the contributions from $c\bar{c}$ production. We have omitted them here to simplify the presentation. This omission is warranted as the $e\mu$ data set proved to be consistent with being entirely due to $b\bar{b}$ production (see Section 6). We define R_Δ as the ratio of the number of sign-subtracted $e\mu$ events after the imposition of all cuts to the number of sign-subtracted $e\mu$ events prior to the imposition of any cuts.

$$R_\Delta \equiv \frac{\Delta_{e\mu}}{\Delta_{e\mu}^{raw}} = \frac{(P)}{(p)}$$

We may obtain R_Δ from the $e\mu$ data set and use it to relate (P) and (p).

$$(P) = R_\Delta (p)$$

The factor, (p), may be written:

$$(p) = \varepsilon_{TRIG} A(be) A(b\mu) \left[\Gamma_{be}\Gamma_{b\mu} + \Gamma_{bce}\Gamma_{bc\mu}\alpha(e)\alpha(\mu) - \Gamma_{be}\Gamma_{bc\mu}\alpha(\mu) - \Gamma_{bce}\Gamma_{b\mu}\alpha(e)\right]$$

where we have defined the ratios:

$$\alpha(e) = \frac{A(bce)}{A(be)}, \ \alpha(\mu) = \frac{A(bc\mu)}{A(b\mu)}$$

and we have used the notation:

$$\Gamma(b \to \ell) \equiv \Gamma_{b\ell}, \ \Gamma(b \to c \to \ell) \equiv \Gamma_{bc\ell} \quad (\ell = e, \mu)$$

The P_T spectrum of indirect leptons is considerably softer than that for direct leptons, meaning that $\alpha(e)$ and $\alpha(\mu)$ are expected to be small. Monte Carlo studies indicate values for $\alpha(\ell)$ of aprroximately 10% (see Section 5). We may then write:

$$(P) = R_\Delta(p) \approx R_\Delta \epsilon_{TRIG} A(be) A(b\mu) \Gamma_{be} \Gamma_{b\mu}$$

$$\sigma(p\bar{p} \rightarrow b\bar{b}\ X) \approx \frac{f_{bb}\Delta_{e\mu}}{\mathcal{L}(1-2\chi)^2 2 R_\Delta \epsilon_{TRIG} A(be) A(b\mu) \Gamma_{be} \Gamma_{b\mu}}$$

The values of χ and the branching fractions are readily available. R_Δ may be found from the $e\mu$ data. The acceptances may be obtained from Monte Carlo. The $b\bar{b}$ fraction, f_{bb}, may be obtained from the $e\mu$ data set via P_T^{rel}. The trigger efficiency is obtainable from a combination of data and simulation.

2 The Electron-Muon Data set

There were two $e\mu$ data sets utilized in this analysis; the data sets differed in size and in the severity of the selection requirements. The "analysis" data set was used to find the number of $b\bar{b} \rightarrow e\mu$ events for the cross section measurement. This data set was created for a previous analysis and its constituent events were selected with relatively tight cuts on the electron and muon candidates. The calculation of a cross section from this set necessitated knowledge of the efficiencies of the cuts placed upon the set. The efficiencies for cuts involving the matching of electron tracks and strip chamber clusters or muon tracks and stubs could have been obtained from conversion electrons and J/ψ's, respectively. The efficiencies for cuts on quantities sensitive to the lepton isolation; however , needed to be obtained for leptons from $b\bar{b}$ production. Ideally, the efficiencies for cuts on variables sensitive to lepton isolation would have been obtained from a version of the analysis data set with looser selection requirements; however, such a data set was obtainable only with great effort. We chose, for the sake of expediency, to create a small set of $e\mu$ events using very loose selection requirements for the purpose of determining the efficiencies of the cuts placed upon isolation sensitive variables. This data set is referred to as the "unbiased" or "raw" $e\mu$ data set.

2.1 The Analysis $e\mu$ Data Set

The analysis data set was a subset of the micro-DST used in the $B^0\overline{B^0}$ mixing analysis [1] The micro-DST was constructed from the CMU04 data stream by selecting events which passed the following requirements:

Event Requirements:

- At least one central electron candidate and at least one muon candidate
- Missing E_T significance less than 2.40
- $| z_{vertex} | < 60cm$
- Run passed BADRUN

Electron Requirements:

- $E_T > 4.0$ GeV

- $\frac{E}{P}$ as calculated from ELES less than 2.0
- $\chi^2_{strip} < 10.0$
- $LSHR < 0.2$
- $\mid \Delta(r\phi) \mid < 2.0cm$
- $\mid \Delta(z) \mid < 3.5cm$
- Cluster is associated with a track

Muon Requirements:

- $P_T > 2.0$ GeV
- Stub matching in $x < 15.0$
- Stub matching in $z < 20.0$
- μ tower $E_{EM} < 2.0$ GeV
- μ tower $E_{HAD} < 4.0$ GeV
- Degree of closest approach of μ track $< 0.5cm$
- Displacement of μ track in z at the distance of closest approach$< 5.0cm$

The analysis data set was culled from the micro-DST by requiring that the event passed the ELECTRON_EMC_5_CMU_3 trigger and that the invariant mass of the electron-muon pair be above 5.0 GeV.

2.2 The Unbiased $e\mu$ Data Set

The unbiased data set was created by culling events from the ELE04 stream that satisified the following requirements:

- A muon candidate with $P_T > 3.0$ GeV and track-stub matching in both the xy and zy planes within 3.5σ of that expected for a muon undergoing multiple scattering
- An electron candidate with $E_T > 4.0$ GeV that is associated with at least one track
- The event passed the ELECTRON_EMC_5_CMU_3 trigger.

3 The Lepton Quality Cuts and The Determination of R_Δ

Cuts were placed upon the electron and muon candidates in the analysis $e\mu$ data sample in order to improve the ratio of signal to noise in the sample. Although the analysis method would work, in principle, with any signal to noise it is to our advantage to reduce the backgrounds as much as possible in order to reduce the experimental error. We are extracting a signal from the difference of two distributions. If the signal is riding upon a large background, the statistical fluctuations in the background will tend to wash out the signal. As mentioned in section 2 some of the cuts placed on the analysis data set are artifacts from the creation of the DST and are not necessarily optimal.

The following cuts were made on the electron candidates in the analysis eμ sample:

- $E_T(e) > E_T^{thresh}(e) \quad (E_T^{thresh}(e) = 5.0\ \mathrm{GeV})$
- $\frac{HAD}{EM} \leq 0.05$
- $\frac{E}{P} \leq 1.4$
- $LSHR < 0.2$
- Only 1 track associated with the cluster and that track is 3D.
- $\Delta(r\phi) \leq 1.5$ cm
- $\Delta(z) \leq 2.5$ cm
- Strip $\chi^2 \leq 10$
- passed FIDELE

The following cuts were made on the muon candidates in the analysis $e\mu$ sample:

- $P_T(\mu) > P_T^{thresh}(\mu) \quad (P_T^{thresh}(\mu) = 3.0, 4.0, 5.0\ \mathrm{GeV})$
- The matching of the CTC track and the muon stub must be within 3σ of that calculated for a muon undergoing multiple scattering.

- The distance of closest approach of the track to the vertex must be less than 50 mm.
- The displacement in z of the track from the vertex must be less than 5 cm at the distance of closest approach.
- The track must consist of at least 40 hits in the CTC.
- The energy deposited in the calorimeter tower to which the track points must be less than 2.0 GeV in the electromagnetic compartment and less than 4.0 GeV in the hadronic compartment.
- passed FIDCMU

It is worth noting that the efficiency of some of the lepton quality cuts are expected to be sensitive to the type of event in which the lepton is embedded and that some are expected to be relatively independent of the leptons origin. In this analysis we are concerned with leptons arising from the semileptonic decay of bottom quarks; such leptons will be associated with the hadronic remnants of the b and will thus be non-isolated. It is necessary then to utilize a sample of leptons with the same or similar isolation as leptons from bs to determine the efficiency of cuts on quantities involving calorimetry. A quantity describing the matching in position between a track and a muon stub, however, is expected to be largely independent of the type of event in which the muon candidate was found. The efficiencies of the muon cuts involving matching the muon track with a stub or a vertex, the 'muon matching cuts', were determined from the J/ψ sample. The efficiencies of the remaining muon cuts and all the electon cuts were determined from the unbiased $e\mu$ sample. Using our previous notation we explicity write the combined cut efficiency as the product of an efficiency dependent upon the lepton origin and an efficiency that is independent of the lepton origin.

$$\epsilon_{CUTS}(i,j) = \epsilon(i,j) \cdot \epsilon_{MATCH} \qquad (i,j) = (be, b\mu), (be, bc\mu), (bce, b\mu), (bce, bc\mu)$$

We must later remember to correct the value of R_Δ for the common term, ϵ_{MATCH}, that has been factored from each of the efficiencies $\epsilon_{CUTS}(i,j)$.

The efficiencies of the matching cuts for muons were determined from events in the $J/\psi \rightarrow \mu^+\mu^-$ sample where both muons were above a 3 GeV P_T threshold. The invariant mass distribution between 2.8 and

3.4 GeV was fittted with a combination of a gaussian and first order polynomial. The number of events falling within one sigma on either side of the J/ψ peak was calulated by integrating the fitted gaussian. The number of actual J/ψ events within this window was determined by subtracting the contribution from the linear background. This procedure was repeated after applying the matching cuts to first one J/ψ leg and then the other. In this manner, the number of legs tested and the number of legs passing each cut could be determined. The efficiencies of the following cuts were found in this manner:

- The matching of the CTC track and the muon stub intercepts, in both the xy and zy planes, must be within 3σ of that calculated for a muon undergoing multiple scattering
- The distance of closest approach of the track to the vertex must be less than 50 mm.
- The displacement in z of the track from the vertex must be less than 5 cm at the distance of closest approach.

The efficiencies for the xy intercept cut and the zy intercept cut were both found to be $(99^{+1}_{-2})\%$, giving a combined efficiency of $(98^{+1}_{-3})\%$. Plots of the xy and zy intercept matching for the events in J/ψ sample are located in Figure 4 and Figure 5 at the end of this section. The efficiency for muon tracks to match the z vertex to within 5 cm was found to be $(99^{+1}_{-2})\%$. The efficiency for a muon track to have a distance of closest approach to the vertex of less than 50 mm was found to be $(100.0^{+0.0}_{-0.2})\%$. Plots of the track Z vertex matching and the distance of closest approach for the events in the J/ψ sample may be found in Figure 6 and Figure 7 at the end of this section. Combining the muon matching efficiencies we find that $\epsilon_{MATCH} = (97^{+2}_{-4})\%$.

The effect of the remaining muon cuts (*i.e.* the minimum ionizing requirements) and all the electron quality cuts are included in the cross section through the term, R_Δ. R_Δ was determined from the unbiased $e\mu$ sample by finding the fraction of the events passing the following cuts:

- The energy deposited in the calorimeter tower to which the muon track points must be less than 2.0 GeV in the electromagnetic compartment and less than 4.0 GeV in the hadronic compartment.
- $\frac{HAD}{EM} \leq 0.05$

- $\frac{E}{P} \leq 1.4$
- $LSHR < 0.2$
- Only 1 track associated with the electron cluster and that track is 3D.
- $\Delta(r\phi) \leq 1.5$ cm
- $\Delta(z) \leq 2.5$ cm
- Strip $\chi^2 \leq 10$

Plots of the quantities mentioned above for the unbiased $e\mu$ sample may be found at the end of this section.

The following table lists the values of R_Δ obtained for three values of the muon P_T threshold:

$E_T^{thresh}(e)$(GeV)	$P_T^{thresh}(\mu)$ (GeV)	R_Δ
5.0	3.0	0.62 ± 0.21
5.0	4.0	0.51 ± 0.17
5.0	5.0	0.40 ± 0.16

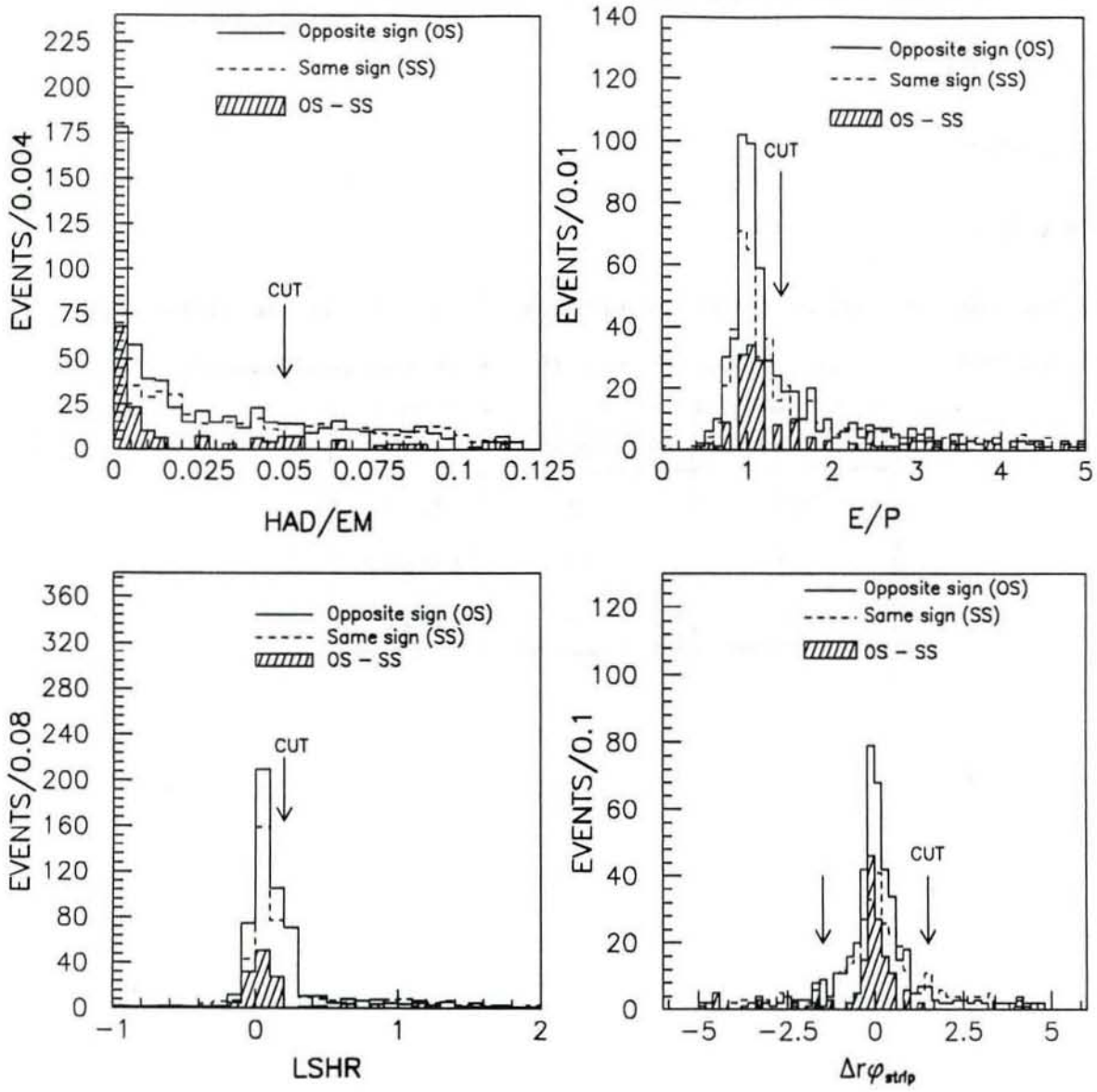

Figure 2: Distributions electron quality variables for the unbiased $e\mu$ sample.

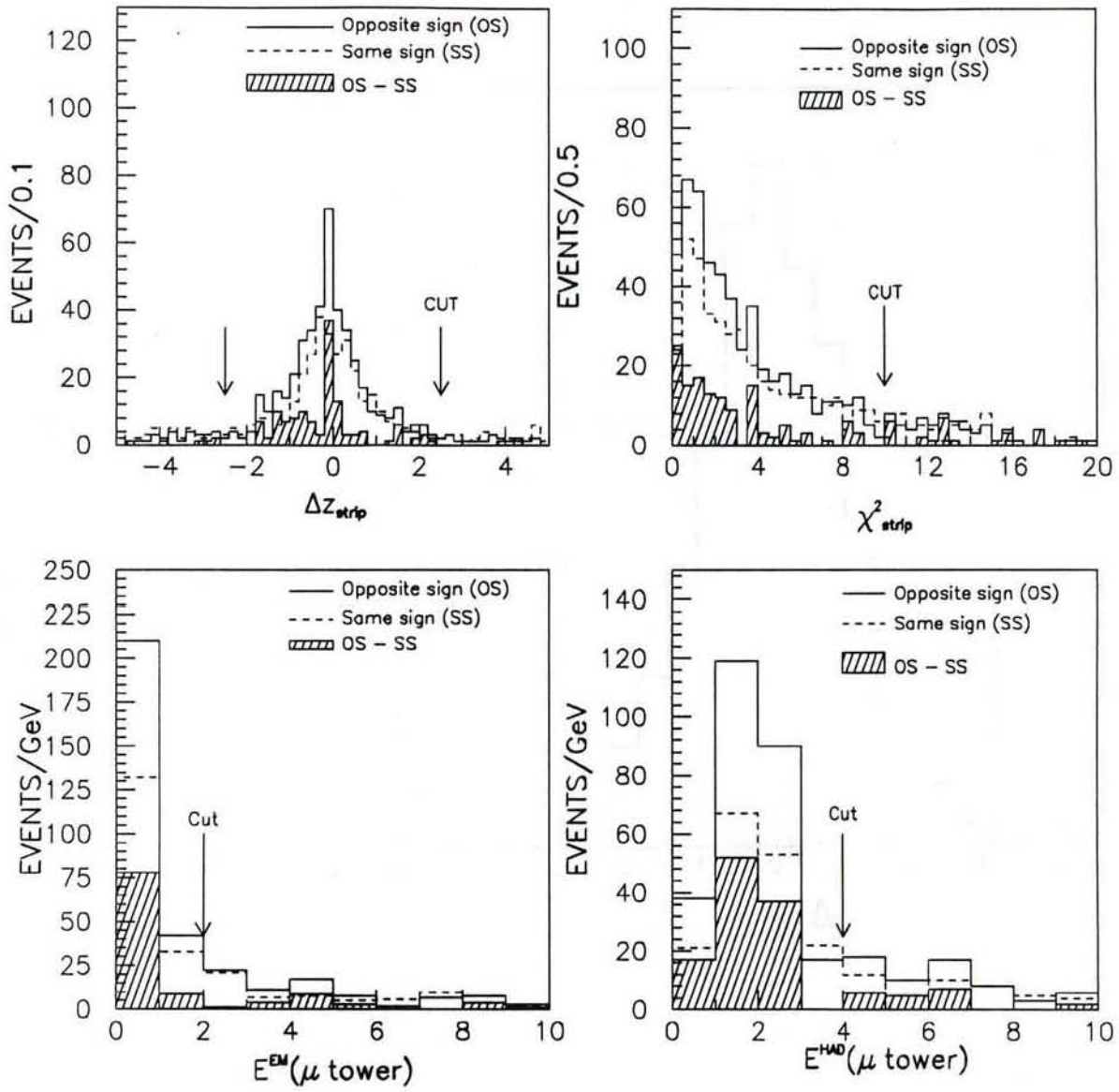

Figure 3: Distributions of electron and muon quality variables for the unbiased $e\mu$ sample.

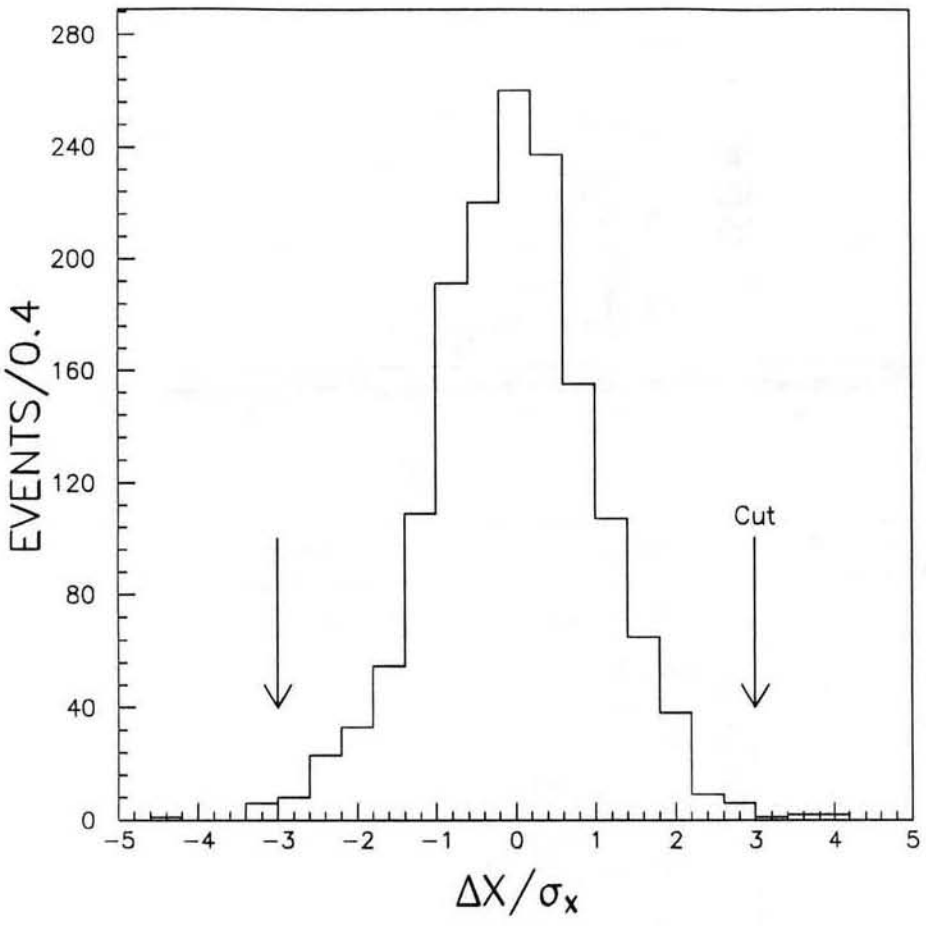

Figure 4: The distribution of track-stub intercept matching in the xy plane for dimuon events within one σ of the J/ψ mass.

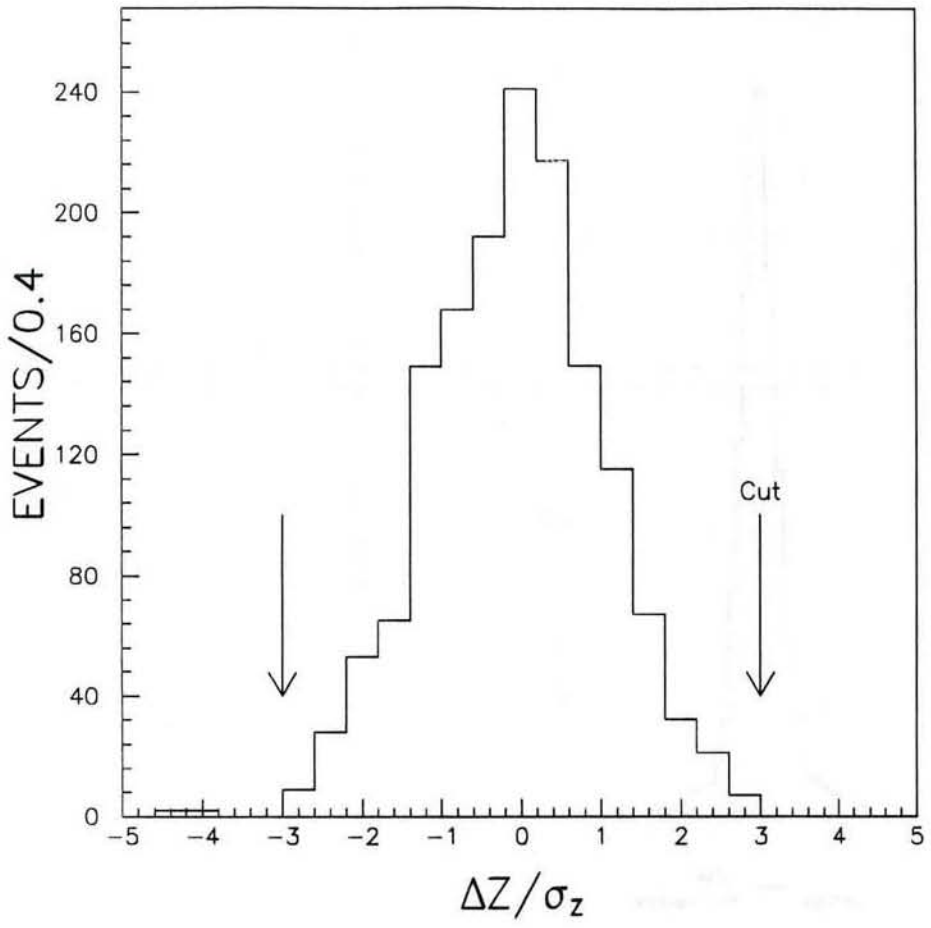

Figure 5: The distribution of track-stub intercept matching in the *zy* plane for dimuon events within one σ of the J/ψ mass.

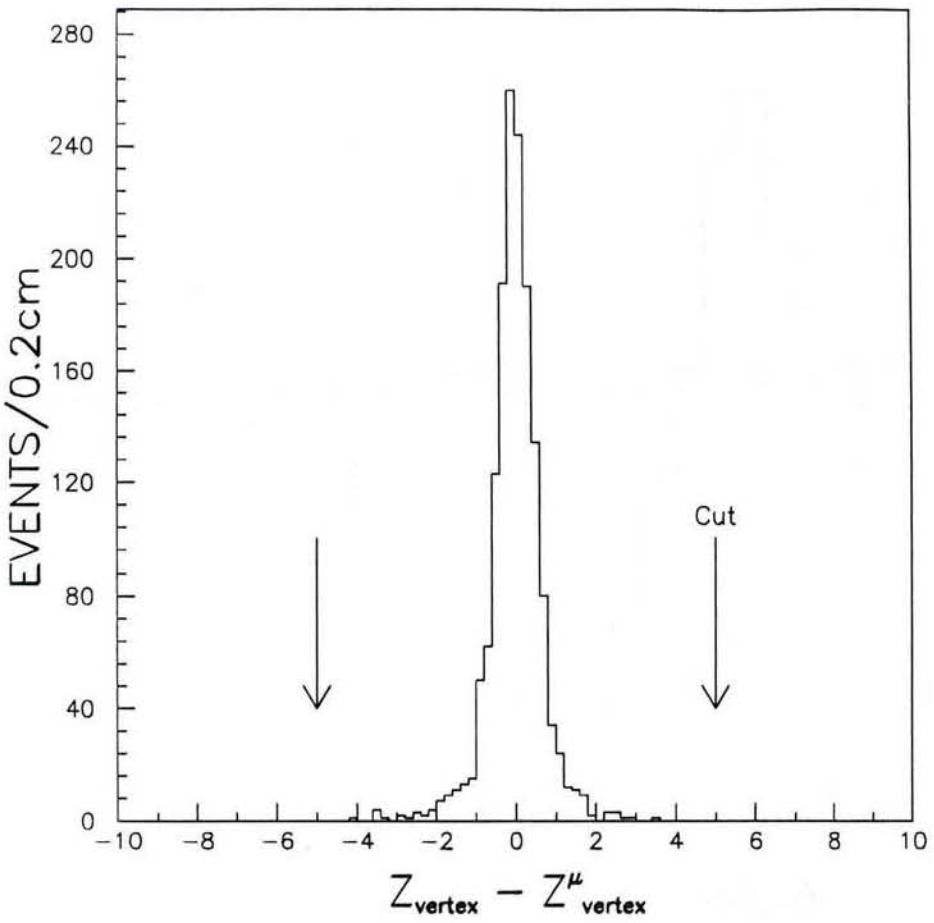

Figure 6: The distance in z of the μ track from the z vertex at the distance of closest approach. The distribution is for dimuon events within one σ of the J/ψ mass

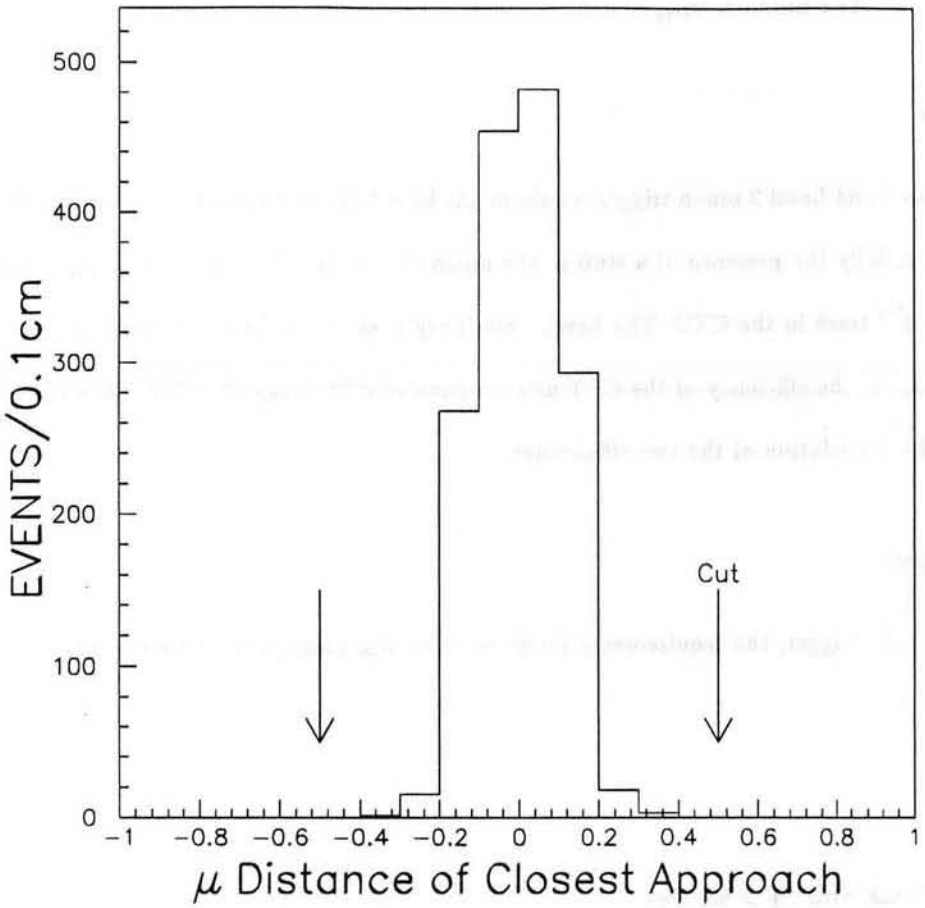

Figure 7: The muon track distance of closest approach. The distribution is for dimuon events within one σ of the J/ψ mass.

4 Trigger Efficiency

The events used in this analysis were required to have passed the ELECTRON_EMC_5_CMU_3 trigger at Level 2. The efficiency of this trigger for $b\bar{b} \rightarrow e\mu$ events was obtained by determining seperately the efficiency of the muon requirements and the efficiency of the electron requirements and considering the total efficiency of the trigger to be their product: $\varepsilon_{trig} = \varepsilon_e \varepsilon_\mu$.

4.1 Muon Trigger

The efficiencies of the Level 1 and Level 2 muon trigger requirements have been measured previously [3]. The Level 1 requirement is essentially the presence of a stub in the muon chambers. The Level 2 requirement is that the stub matches a CFT track in the CTC. The Level 1 efficiency is shown in Figure 8 as a function of CTC track P_T. Figure 9 shows the efficiency of the CFT as a function of CTC track P_T. The muon trigger efficiency is taken to be the convolution of the two efficiencies.

4.2 Electron Trigger

For the electron portion of the trigger, the requirements made upon an electromagnetic cluster were:

- $E_T > 5.0$ GeV
- $\frac{HAD}{EM} < 0.125$
- An associated CFT track with $P_T > 4.8$ GeV

The first two requirements may be considered as constituting an electron calorimeter efficiency and the last requirement an electron tracking efficiency. The electron tracking efficiency was determined previously [4] and is shown in Figure 10.

The electron calorimeter efficiency for electrons from bottom decays was determined from Monte Carlo. ISAJET was used to generate $b\bar{b}$ events where one bottom quark decayed to an electron and the other quark decayed to a muon. The events were passed through QFL, TRGSIM, and the usual electron and muon reconstruction code. The trigger efficiency was determined from events for which the invariant mass of the

electron-muon pair was above 5.0 GeV and the P_T of the muon was above the appropriate threshold. The electron calorimeter efficiency thus obtained is shown in Figure 11 as a function of the reconstructed electron E_T. It should be noted that the trigger E_T and the reconstructed E_T are not usually the same as the trigger and the offline reconstruction code use different tower sizes for clustering. The turn-on of the trigger efficiency is due to the trigger E_T threshold requirement whereas the asymptotic efficiency is dominated by the trigger requirement upon the $\frac{HAD}{EM}$. The effect of the trigger E_T threshold is largely due the previously mentioned difference in the trigger and offline clustering , the trigger's assumption that the z vertex is at zero when calculating transverse energies, and the difference in the trigger and DAQ energy response. The effect of the clustering difference and vertex smearing is expected to be reasonably well modelled by the simulation. The resolution function relating the transverse energy response of the trigger and the DAQ system has been previously measured [4] and was included in the trigger simulation. It is not obvious that the effect of the $\frac{HAD}{EM}$ requirement is well modelled. To build confidence in the simulation, we investigated the electron isolation. Two isolation variables were used: the track isolation was defined as the scalar sum of the P_T of the tracks in a cone of radius 0.5 centered on the electron and excluding the eletron, the calorimeter isolation was defined as the sum scalar E_T in a cone of radius 0.4 centered on the electron minus the E_T of the electron. Figure 12 shows the comparison between the sign-subtracted track isolation distribution for electrons from the data and the track isolation distribution for simulated electrons. Figure 13 shows the comparison between the sign-subtracted calorimeter isolation distribution for electrons from the data and the calorimeter isolation distribution for simulated electrons. For both comparisons, the simulated electrons were subjected to the same cuts as the data. The isolation distributions from the simulation are seen to compare well with those from the data.

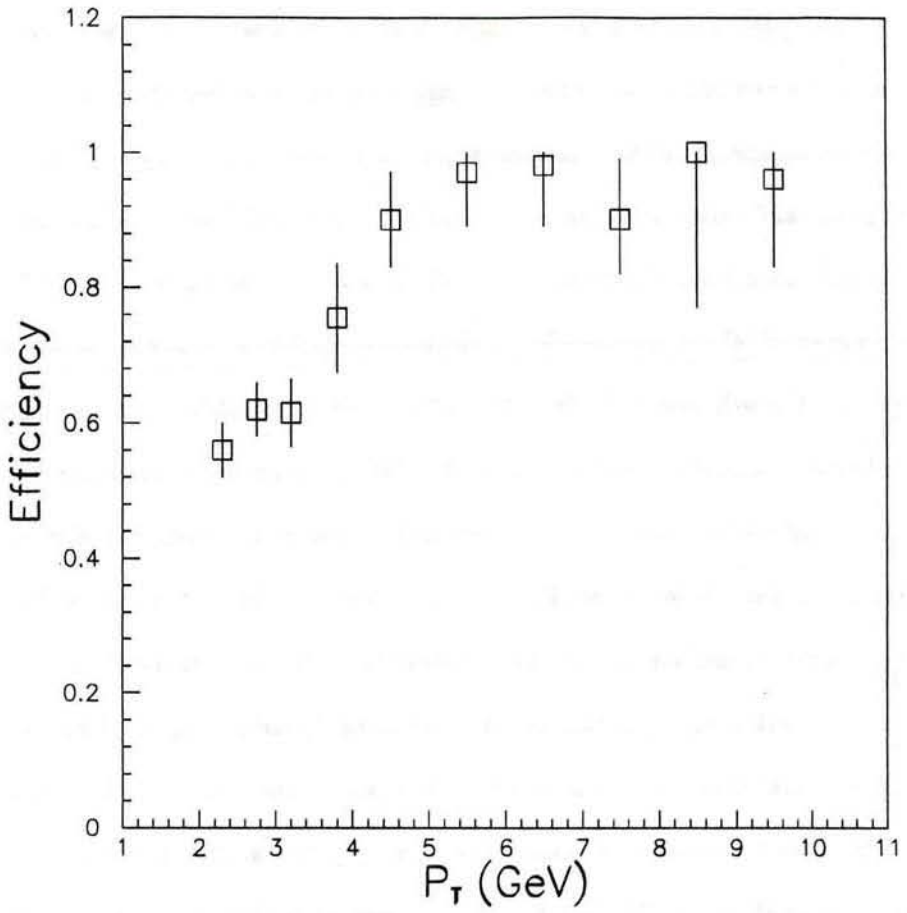

Figure 8: The efficiency of the Level 1 muon trigger as a function of the CTC track P_T (from Reference [3]).

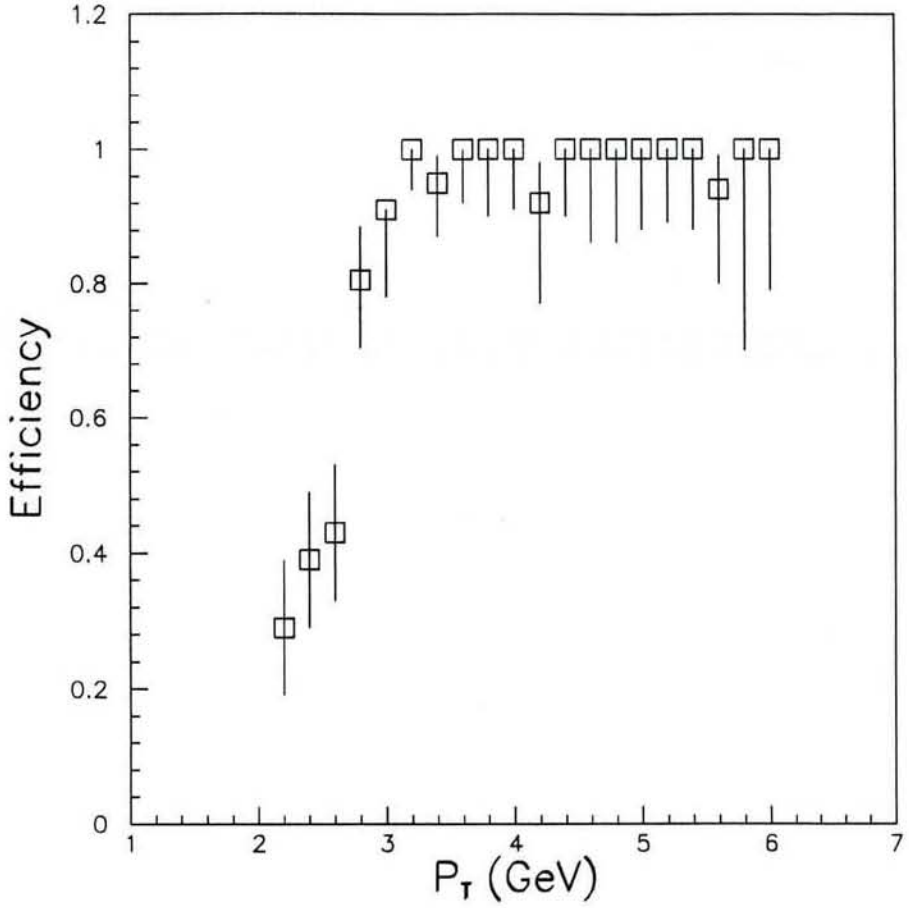

Figure 9: The efficiency of the Level 2 muon trigger as a function of the CTC track P_T (from Reference [3]).

Figure 10: **The electron tracking efficiency as a function of the CTC track P_T** (from reference [4]).

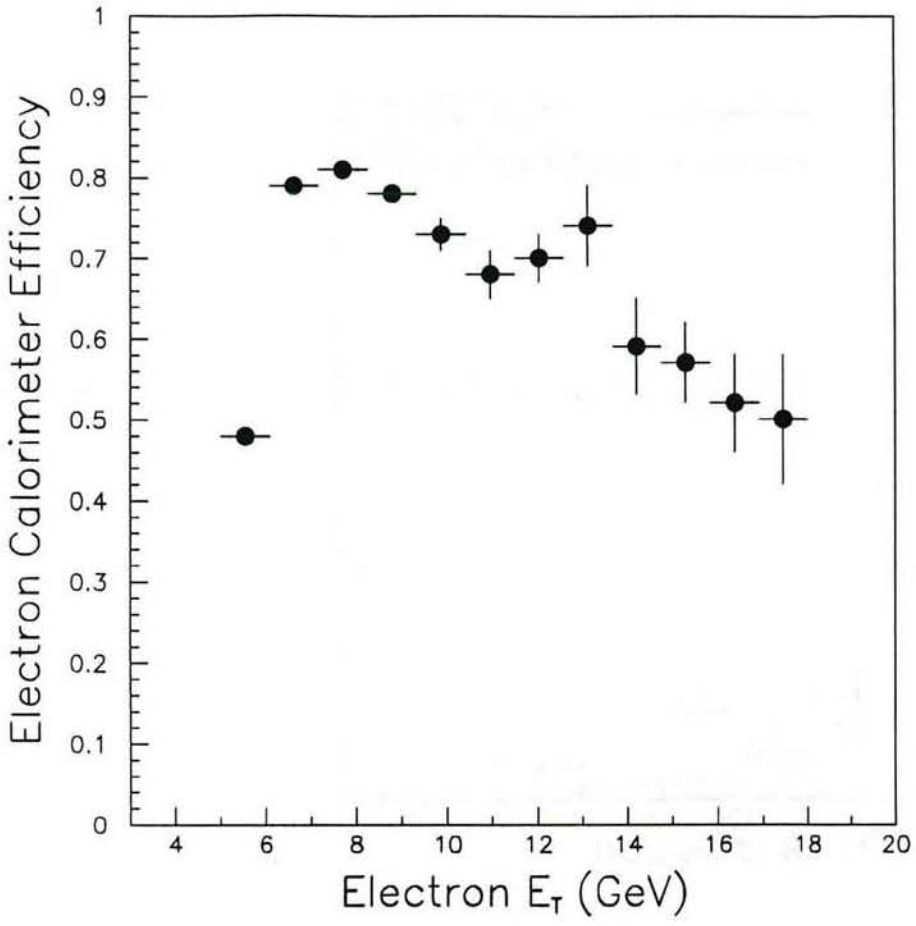

Figure 11: The electron calorimeter efficiency as a function of the reconstructed E_T of the electron. The results shown were obtained from ISAJET plus the QFL detector simulation.

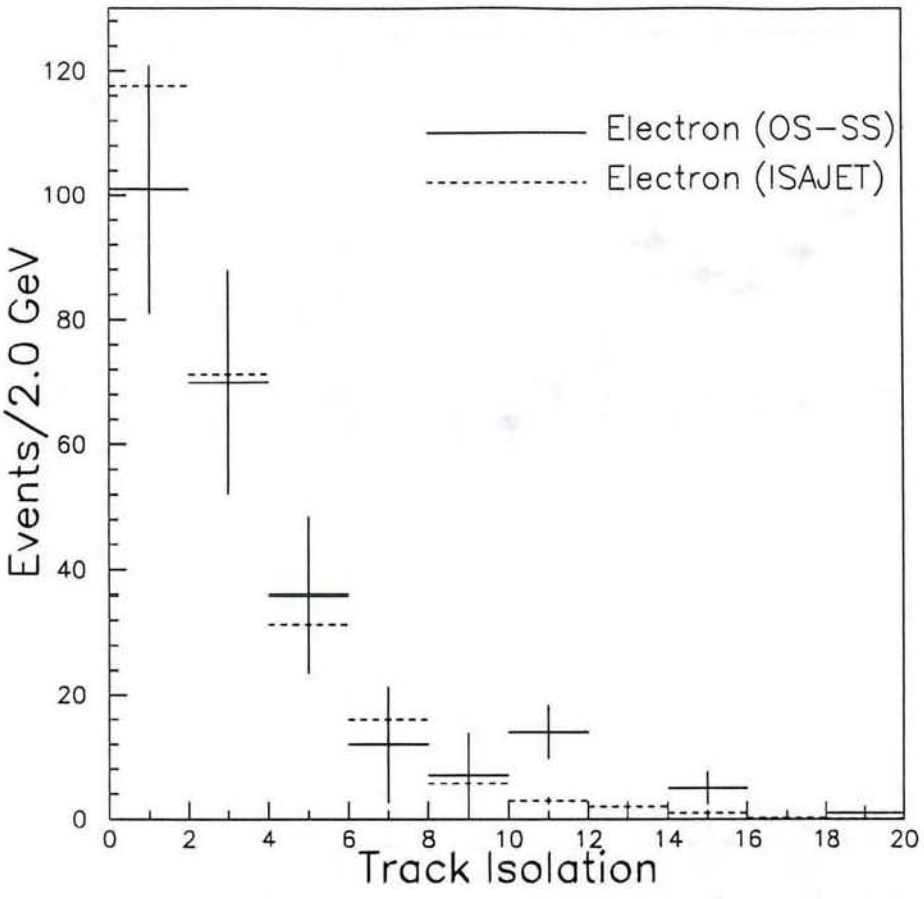

Figure 12: A comparison of the opposite sign minus same sign electron isolation as seen in the analysis data set and the electron isolation from Monte Carlo with the same cuts. The Monte Carlo distribution is normalized to the number of events from the data.

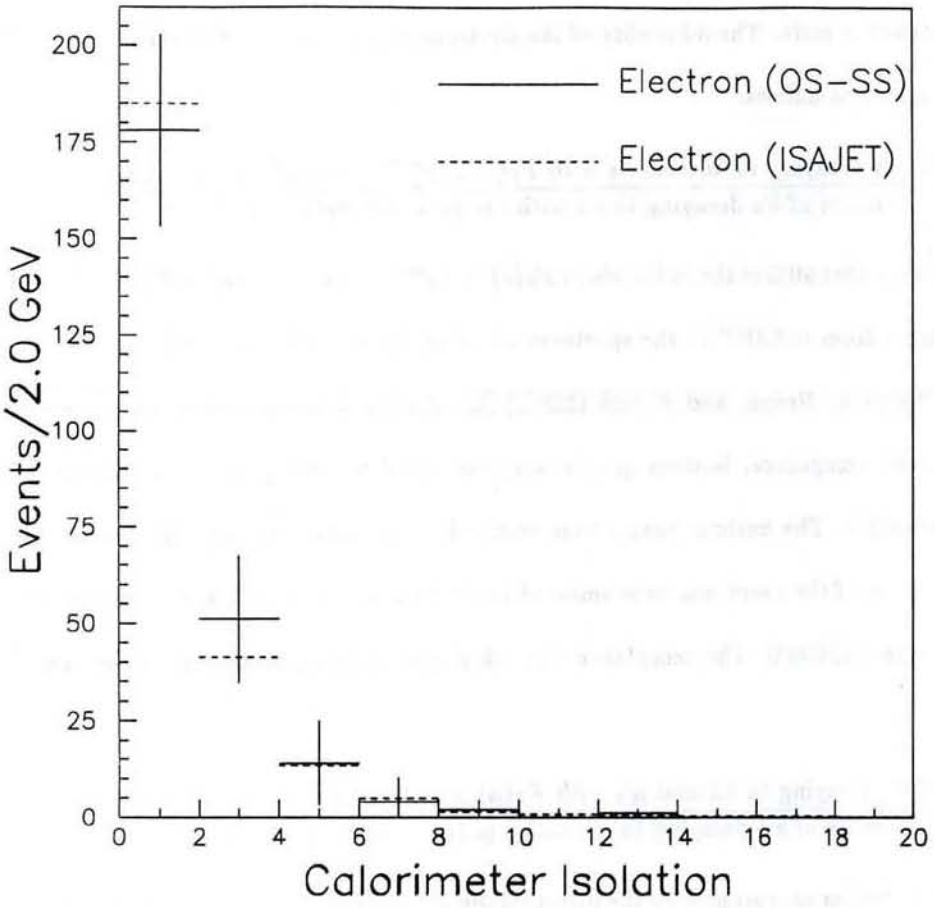

Figure 13: A comparison of the opposite sign minus same sign muon isolation as seen in the analysis data set and the muon isolation from Monte Carlo with the same cuts. The Monte Carlo distribution is normalized to the number of events from the data.

5 Acceptances

The acceptances for electrons and muons were obtained from Monte Carlo. The electron acceptance was determined from ISAJET lowest order $b\bar{b}$ production. Bottom quarks were generated with $\mid y_b \mid < 1$ and were required to decay directly to an electron. The events were then simulated with QFL and subjected to the usual electron reconstruction code. The fiduciality of the electrons was tested with the routine FIDELE. The acceptance was calculated as follows:

$$A(be) = \frac{\text{Number of } b\text{'s decaying to fiducial } e\text{'s with } P_T(e) > P_T^{thresh}(e) \text{ and } \mid z_{vertex} \mid < 60cm}{\text{Number of } b\text{'s decaying to } e\text{'s with } \mid y_b \mid < 1 \text{ and } P_T(b) > P_T^{min}}$$

P_T^{min} is defined as the P_T such that 90% of the bs for which $P_T(e) > P_T^{thresh}(e)$ have $P_T(b) > P_T^{min}$. Figure 14 compares the b P_T spectrum from ISAJET to the spectrum obtained from the Monte Carlo calculation of NLO $b\bar{b}$ production by Mangano, Nason, and Ridolfi (MNR) [5]. As the figure indicates, the agreement is quite good. For the muon acceptance, bottom quarks were generated according to the appropriate P_T spectrum as obtained from MNR. The bottom quarks were required to be within unit rapidity and to decay directly to a muon. The vertex of the event was then smeared in z by a gaussian of $\sigma = 30cm$ and the muon was tested for fiduciality with FIDCMU. The acceptance was calculated in the same manner as the electron acceptance:

$$A(b\mu) = \frac{\text{Number of } b\text{'s decaying to fiducial } \mu\text{'s with } P_T(\mu) > P_T^{thresh}(\mu) \text{ and } \mid z_{vertex} \mid < 60cm}{\text{Number of } b\text{'s decaying to } \mu\text{'s with } \mid y_b \mid < 1 \text{ and } P_T(b) > P_T^{min}}$$

The ratios of the indirect lepton acceptances to the direct lepton acceptances were calculated in the same manner as the respective direct lepton acceptance.

$$\alpha(\mu) \equiv \frac{A(bc\mu)}{A(b\mu)}, \quad \alpha(e) \equiv \frac{A(bce)}{A(be)}$$

The values obtained for the acceptances and ratios of acceptances are listed in the following table (the errors are due to Monte Carlo statistics):

P_T^{thresh} (GeV)	P_T^{min} (GeV)	$A(b\mu)$	$\alpha(\mu)$
3.0	6.50	0.157 ± 0.001	0.182 ± 0.006
4.0	7.50	0.122 ± 0.001	0.130 ± 0.008
5.0	8.75	0.097 ± 0.001	0.126 ± 0.010
E_T^{thresh} (GeV)	P_T^{min} (GeV)	$A(be)$	$\alpha(e)$
5.0	8.75	0.144 ± 0.003	0.099 ± 0.004

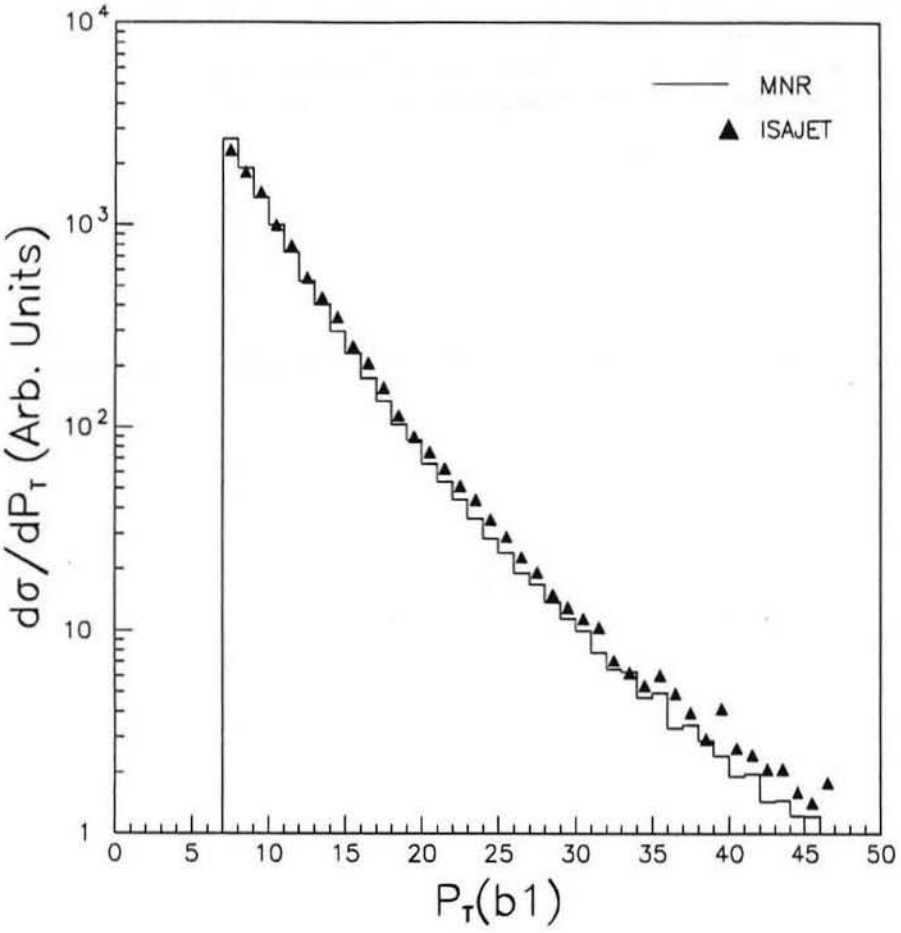

Figure 14: A comparison of b P_T spectra from MNR and ISAJET.

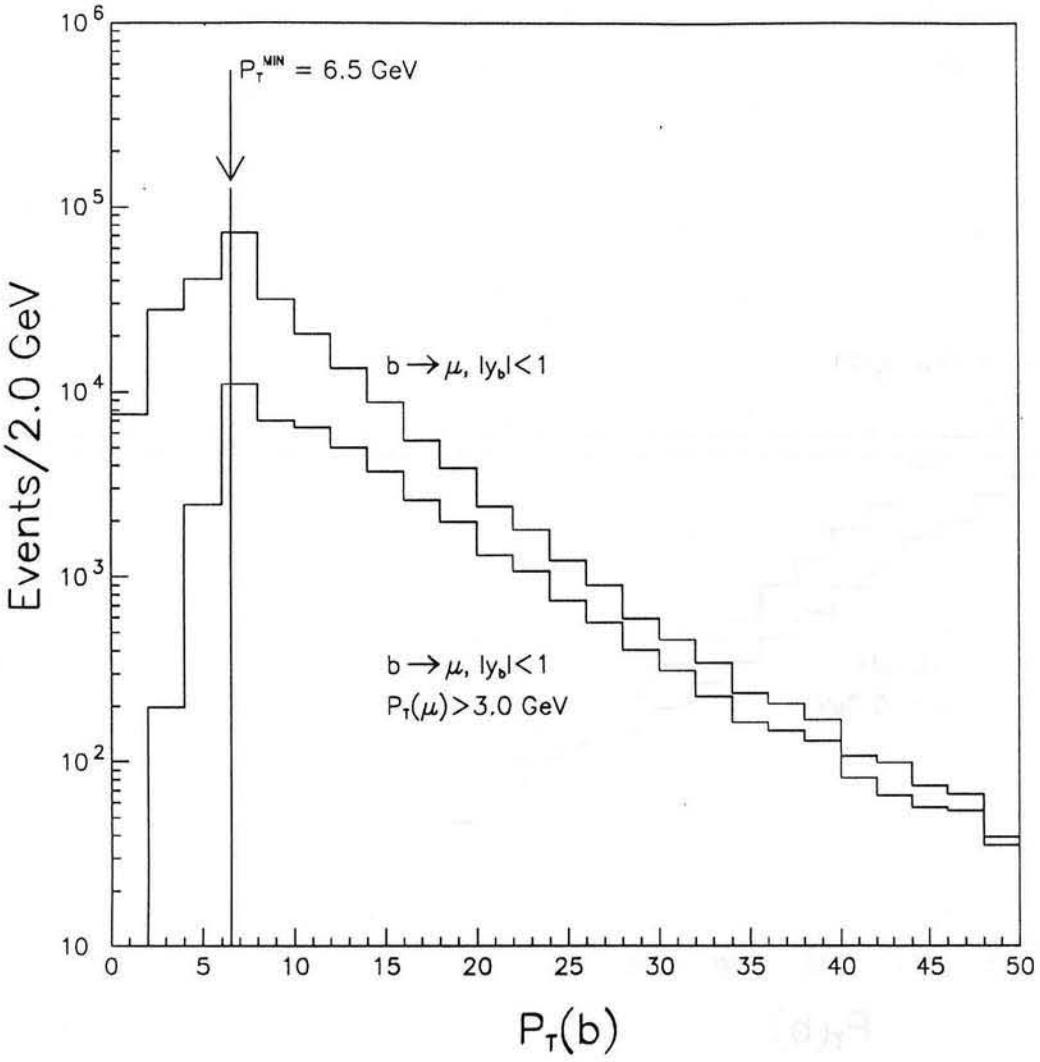

Figure 15: P_T for all bs generated with $|\ y_b\ | < 1$ and that produce a μ (*upper*) and the subset of those for which $P_T(\mu) > 3.0$ GeV. (*lower*).

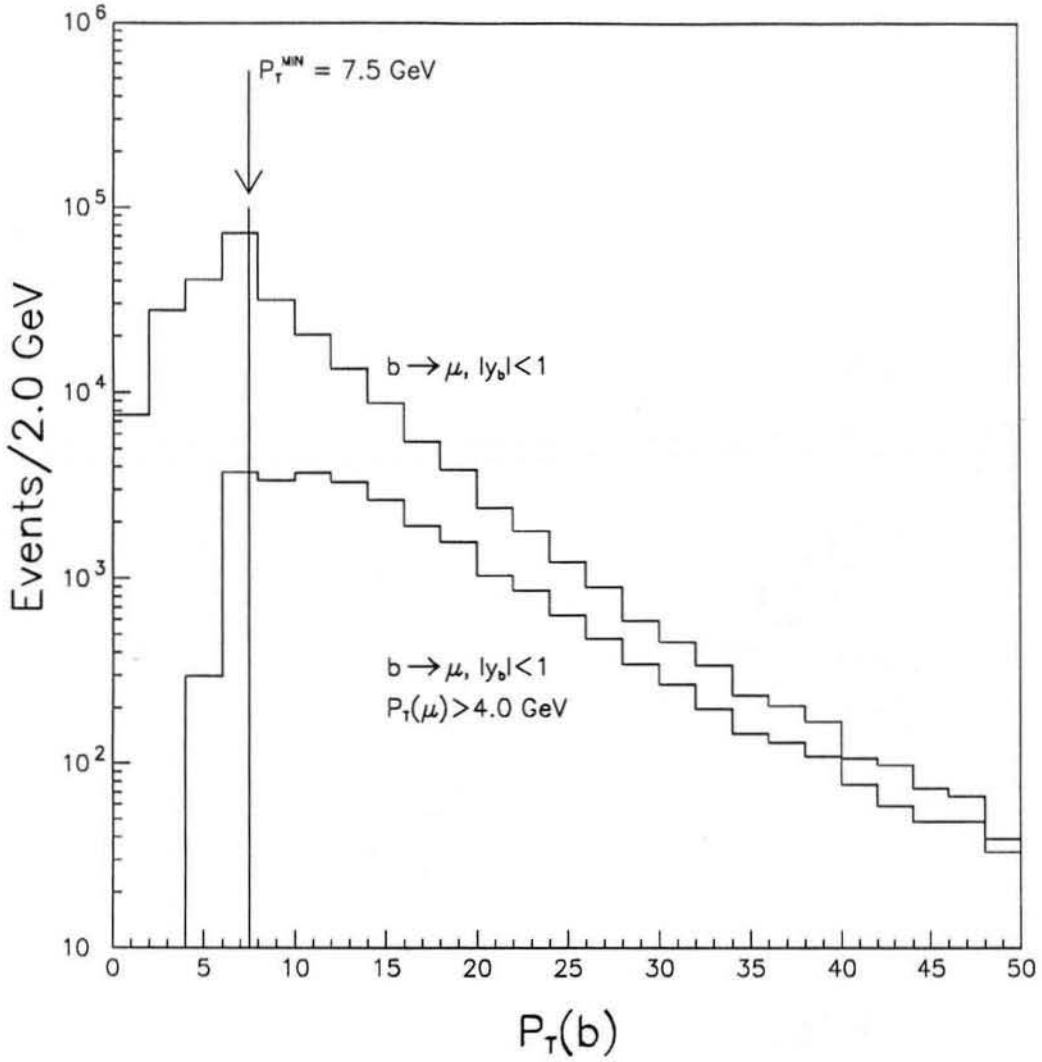

Figure 16: P_T **for all** b**s generated with** $|\ y_b\ | < 1$ **and that produce a** μ (*upper*) **and the subset of those for which** $P_T(\mu) > 4.0$ **GeV.** (*lower*).

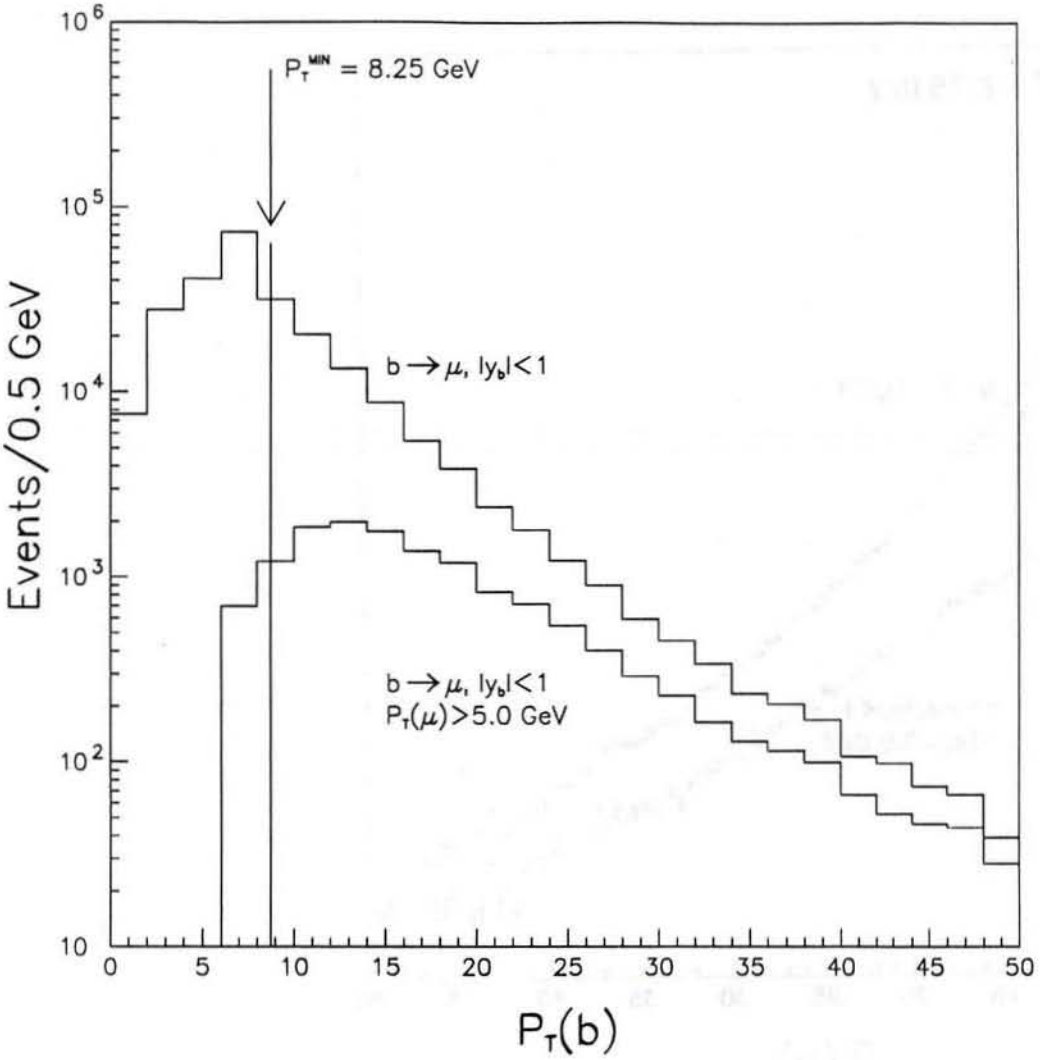

Figure 17: P_T for all bs generated with $| y_b | < 1$ and that produce a μ (*upper*) and the subset of those for which $P_T(\mu) > 5.0$ GeV (*lower*).

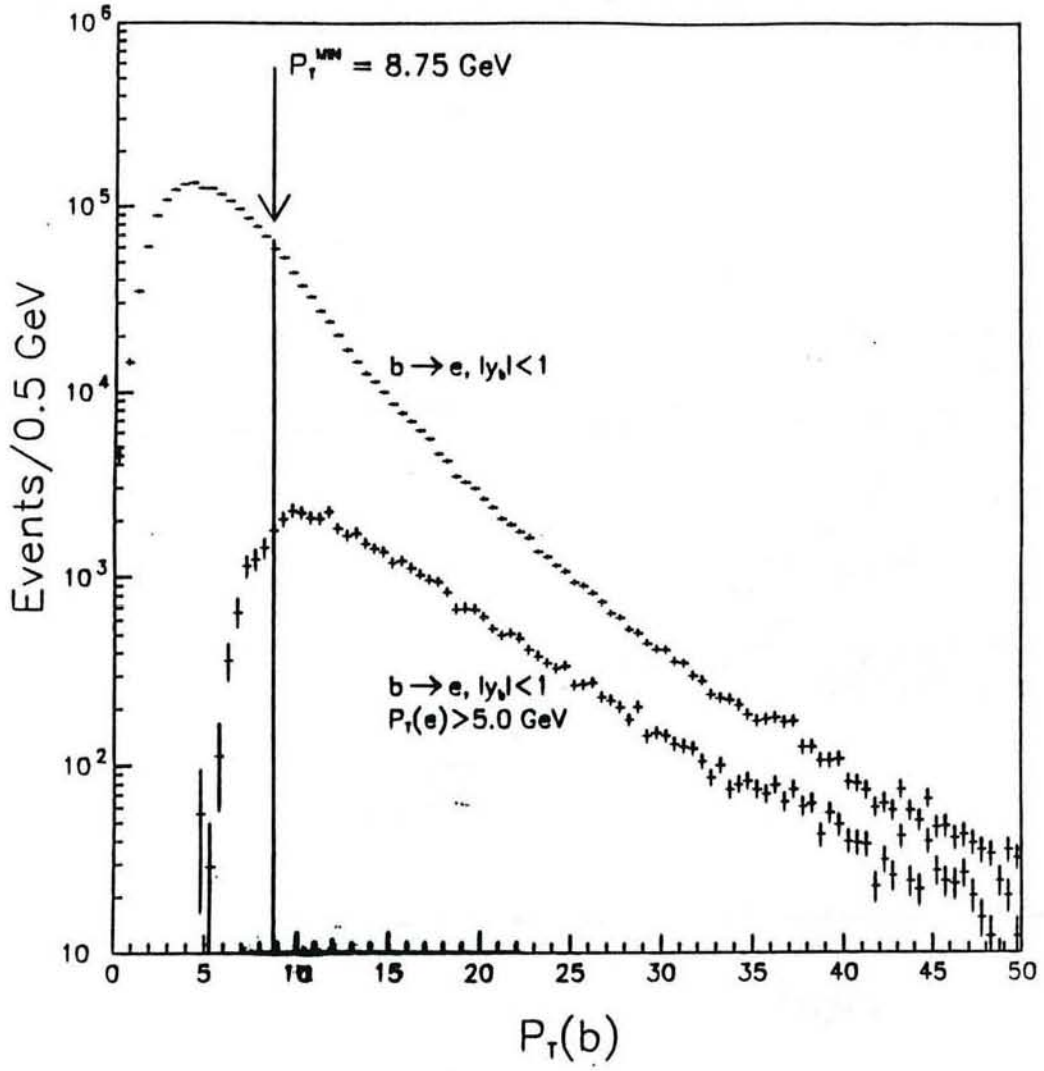

Figure 18: P_T for all bs generated with $\mid y_b \mid < 1$ and that produce an electron (*upper*) and the subset of those for which $P_T(e) > 5.0$ GeV. (*lower*).

6 Determining $f_{b\bar{b}}$

Knowledge of the number of $b\bar{b}$ events in the analysis $e\mu$ sample after all cuts have been imposed is necessary for the calculation of the $b\bar{b}$ cross section. Recalling the discussion in section 1.4, the $b\bar{b}$ content of the sample enters into the cross section through the term, $f_{b\bar{b}}$, where:

$$f_{b\bar{b}} = \frac{\Delta_{b\bar{b}}}{\Delta_{e\mu}} = \frac{N^{os}_{b\bar{b}} - N^{ss}_{b\bar{b}}}{N^{os}_{e\mu} - N^{ss}_{e\mu}}$$

$N^{os}_{e\mu}, N^{ss}_{e\mu}, N^{os}_{b\bar{b}}, N^{ss}_{b\bar{b}}$ refer to the number of *os* and *ss* $e\mu$ events after all cuts, and the number of those events due to $b\bar{b}$ production. This fraction can be determined from the data set by examining the distribution of a variable expected to differ in shape for $c\bar{c}$ and $b\bar{b}$ events. The distribution of this variable for the data set will be a combination of the $c\bar{c}$ shape and the $b\bar{b}$ shape. Fitting the distribution with the sum of normalized $b\bar{b}$ and $c\bar{c}$ shapes obtained from Monte Carlo will give us the $b\bar{b}$ and $c\bar{c}$ content.

In this analysis, the variable used to obtain seperation between $b\bar{b}$ and $c\bar{c}$ was the P_T of the lepton relative to the axis of the associated jet, P_T^{rel}.

$$P_T^{rel} = P_\ell sin(\theta_{\ell-jet})$$

The relative P_T is calculated as the magnitude of the lepton momentum times the sine of the angle between the lepton direction and the axis of the associated jet. The P_T^{rel} distribution for leptons from b decays is expected to be stiffer than that for c decays because leptons from bs tend to be more energetic and because of the larger opening angle between the lepton and the hadronic remnants due to the greater b mass.

The P_T^{rel} distributions for leptons from b and c decays were obtained from Monte Carlo. $b\bar{b}$ and $c\bar{c}$ events were generated with ISAJET and simulated with QFL. The simulated events were then subjected to the same cuts as the $e\mu$ data. The P_T^{rel} distributions obtained from the Monte Carlo were parametrized by fitting them with the functional form $Cx^\alpha exp(\frac{x^\beta}{\gamma})$. The normalized parametrizations for $c\bar{c}$ and $b\bar{b}$ are compared in Figure 19 and Figure 20.

The P_T^{rel} distributions for the $e\mu$ data set after all cuts are shown in Figure 21 and Figure 22. The figures show distributions for *os* pairs and *ss* pairs. To determine $f_{b\bar{b}}$ we fit the difference of the *os* and *os* distributions with the weighted sum of the normalized P_T^{rel} parametrizations for $b\bar{b}$ and $c\bar{c}$. The weights

were expressed in terms of the sole fit parameter, $f_{b\bar{b}}$, with the $b\bar{b}$ weighting being given by $f_{b\bar{b}}$ and the $c\bar{c}$ weighting by $1 - f_{b\bar{b}}$:

$$f_{b\bar{b}} P_T^{rel}(b) + (1 - f_{b\bar{b}}) P_T^{rel}(c)$$

The likelihood fit to the electron $P_T^{rel}(os - ss)$ distribution is shown in Figure 23. The fit parameter P1 corresponds to $f_{b\bar{b}}$. The likelihood fit to the muon $P_T^{rel}(os - ss)$ distribution is shown in Figure 24.

As indicated in the figures, the difference distributions are consistent with being due solely to $b\bar{b}$. We find that: $f_{b\bar{b}} = 1.0$ with an estimated error of 15%.

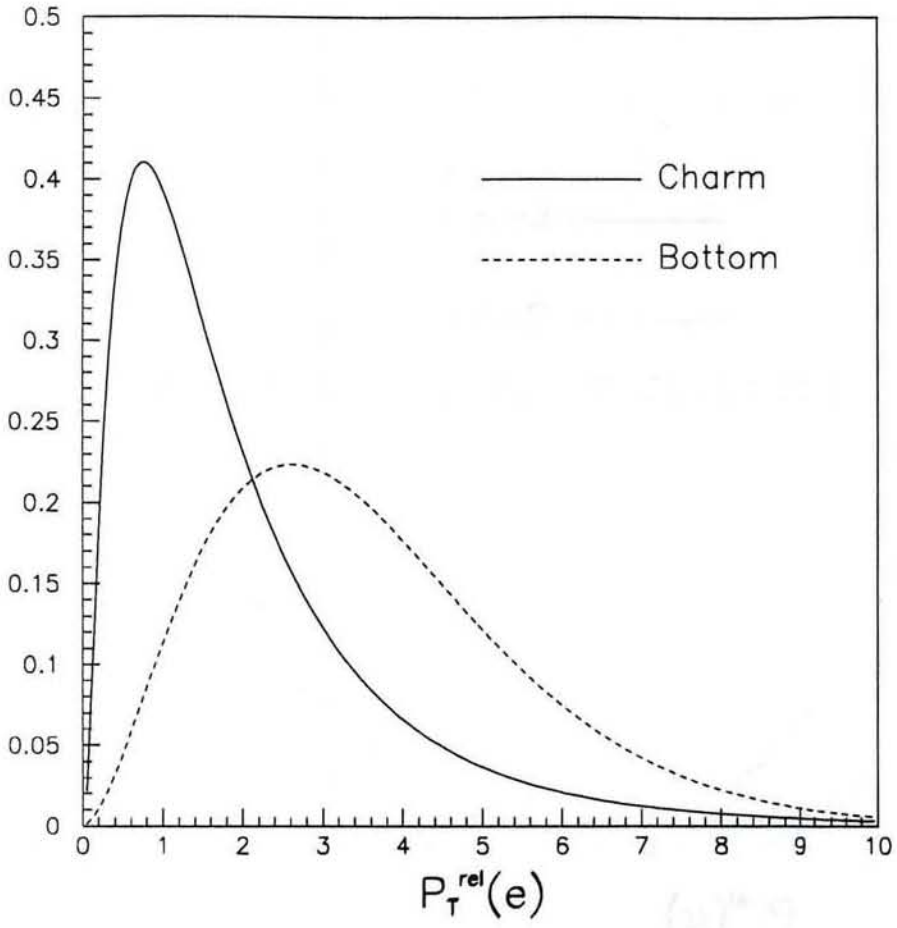

Figure 19: A comparison of the normalised P_T^{rel} shapes for electrons from charm and from bottom quarks. The curves are parametrizations of distributions from ISAJET after the imposition of all analysis cuts.

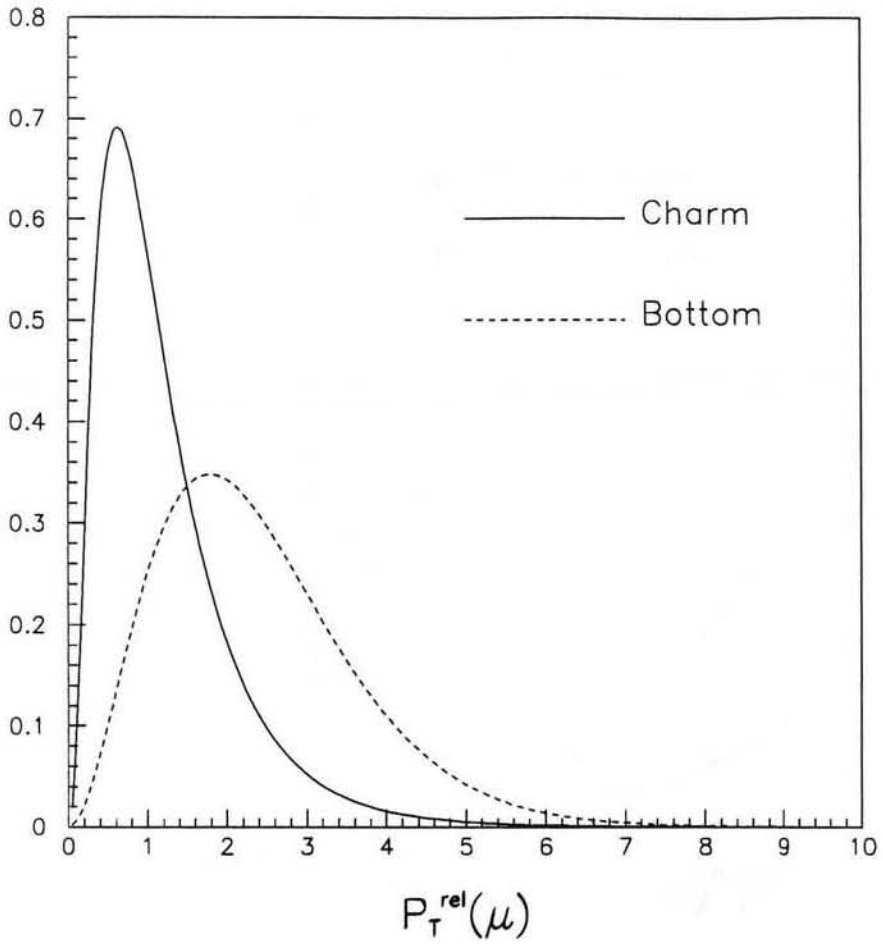

Figure 20: A comparison of the normalized P_T^{rel} shapes for muons from charm and from bottom quarks. The curves are parametrizations of distributions from ISAJET after the imposition of all analysis cuts.

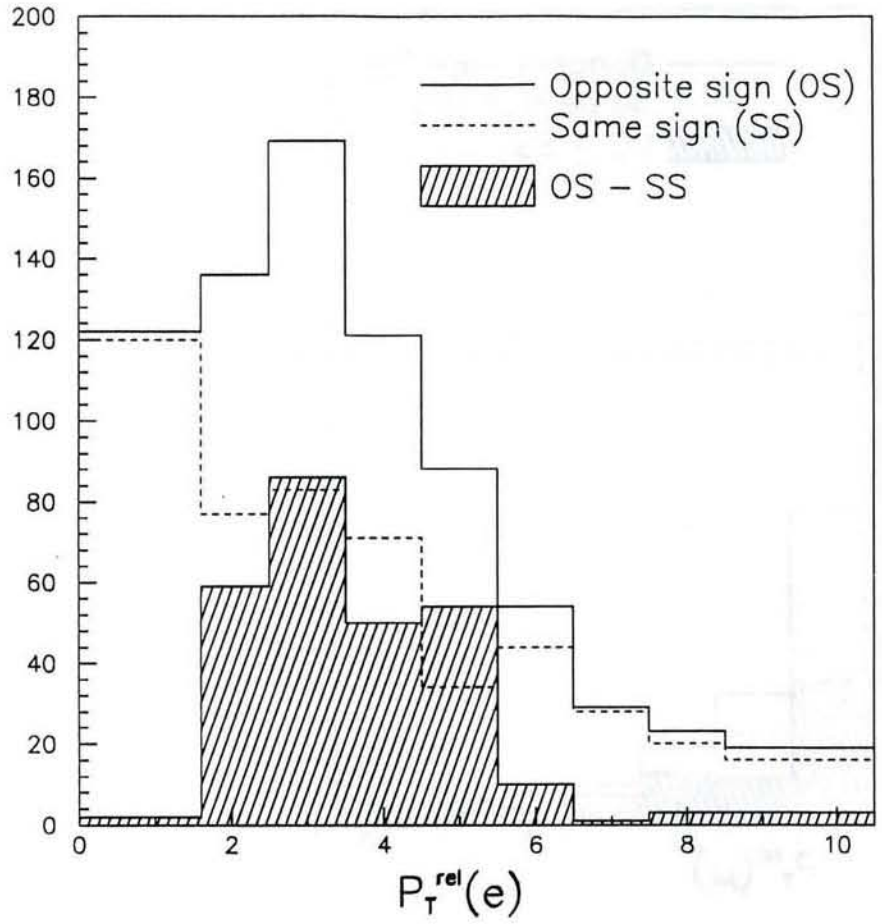

Figure 21: The P_T^{rel} distribution for electrons in the $e\mu$ sample.

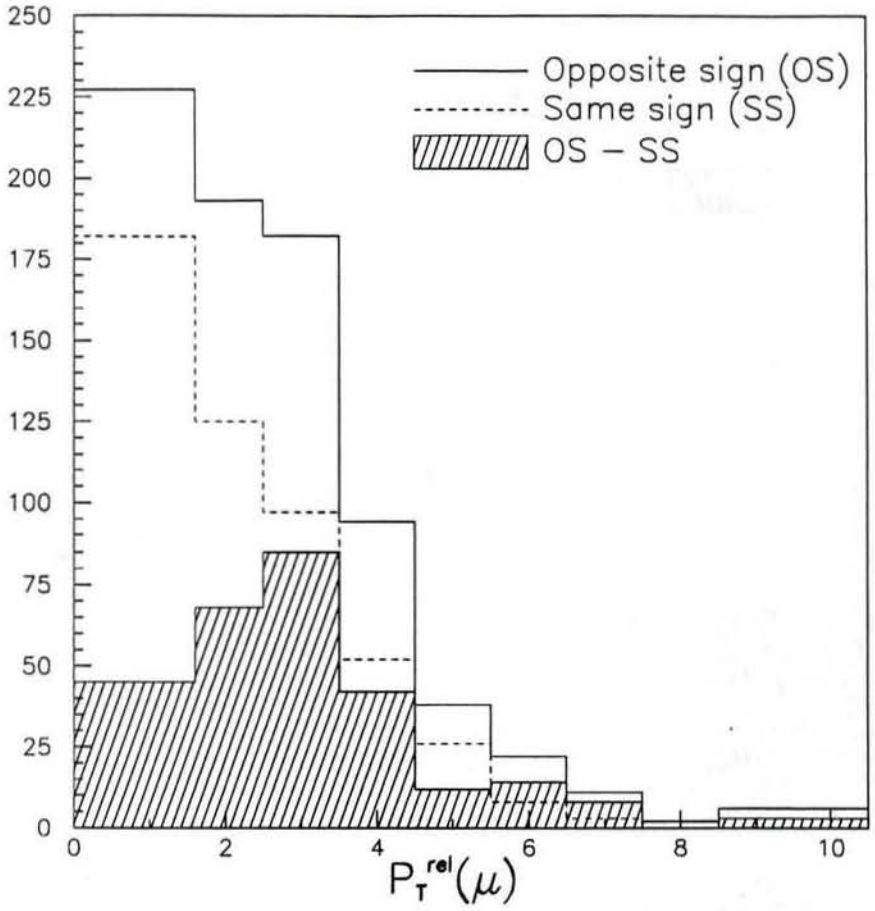

Figure 22: The P_T^{rel} distribution for muons in the $e\mu$ sample.

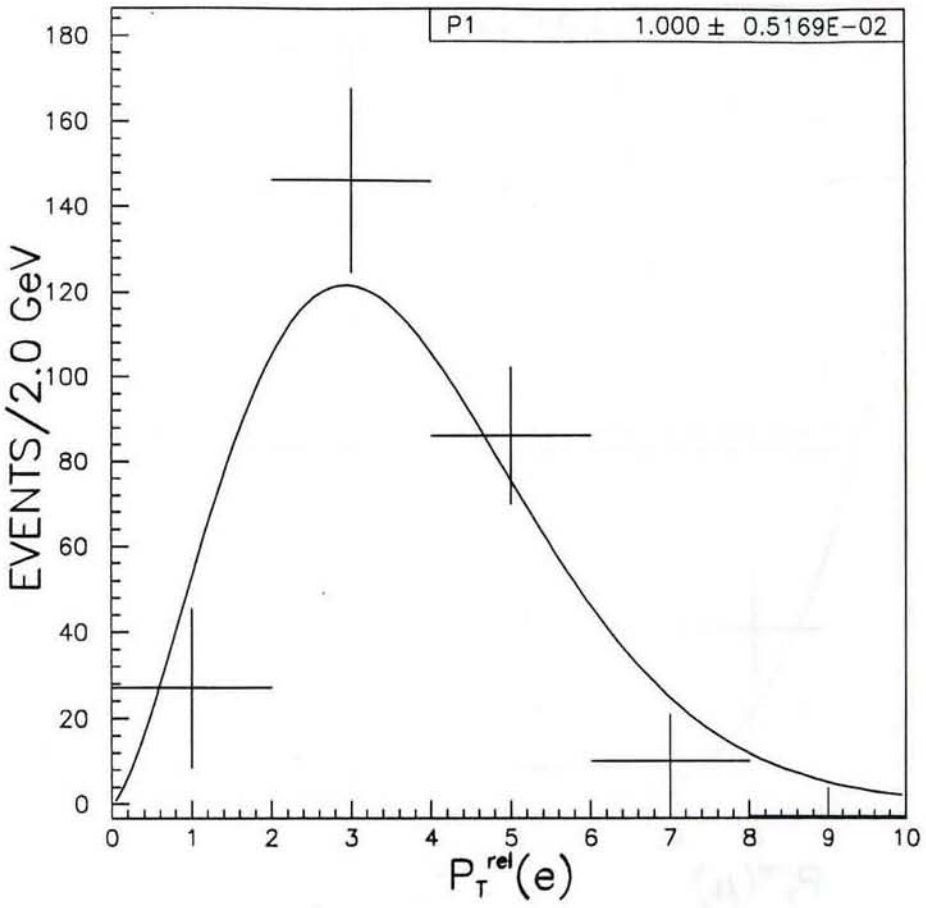

Figure 23: Result of likelihood fit to the *os* minus *ss* P_T^{rel} distribution for electrons. The functional form used was: $(P1)P_T^{rel}(b) + (1 - P1)P_T^{rel}(c)$ where $P_T^{rel}(b)$ and $P_T^{rel}(c)$ represent the normalized parametrizations of the relative P_T distributions for electrons from $b\bar{b}$ and $c\bar{c}$ as obtained from ISAJET. The fit parameter, $P1$, represents the $b\bar{b}$ fraction, $f_{b\bar{b}}$.

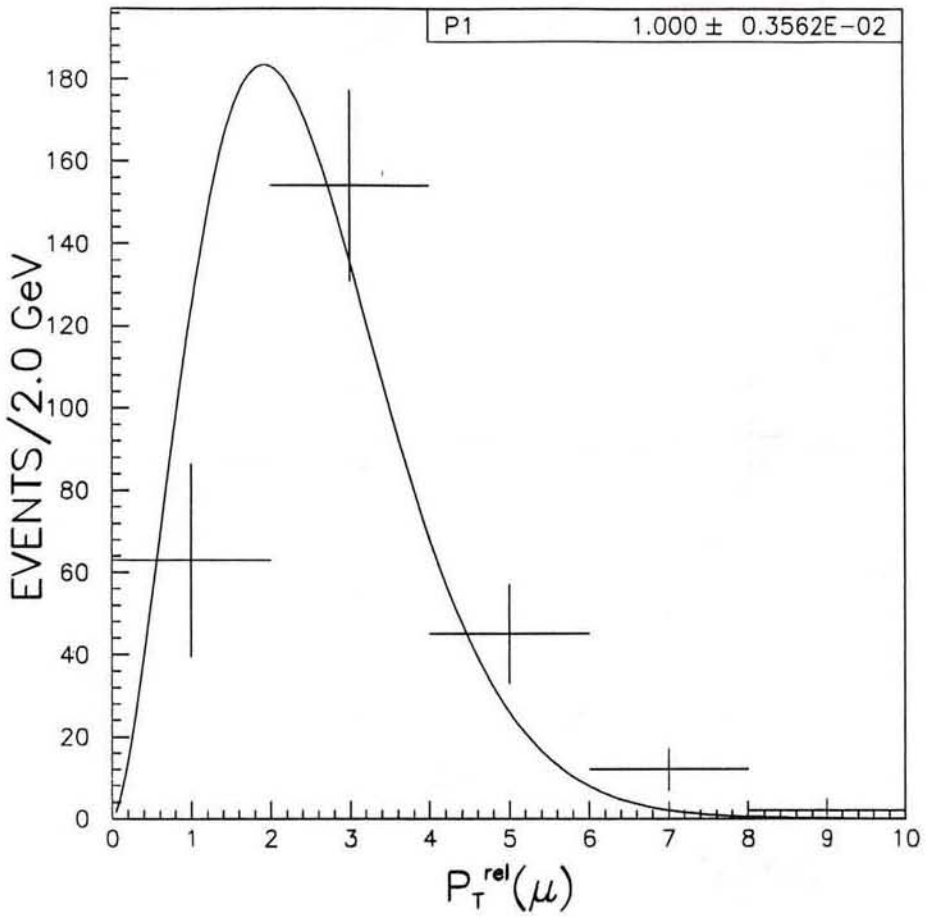

Figure 24: Result of likelihood fit to the *os* minus *ss* P_T^{rel} distribution for muons. The functional form used was: $(P1)P_T^{rel}(b) + (1 - P1)P_T^{rel}(c)$ where $P_T^{rel}(b)$ and $P_T^{rel}(c)$ represent the normalized parametrizations of the relative P_T distributions for muons from $b\bar{b}$ and $c\bar{c}$ as obtained from ISAJET. The fit parameter, $P1$, represents the $b\bar{b}$ fraction, $f_{b\bar{b}}$.

7 $\sigma(b\bar{b}\ X)$

The following tables list the quantities relevant to the measurement of $\sigma(b\bar{b}\ X)$:

Factor	*Value*
f_{bb}	$1.0^{+0.00}_{-0.15}$
χ	0.16 ± 0.04
$\mathcal{L}$	$2.65 \pm .17\ pb^{-1}$
$A(be)$	0.144 ± 0.003
$\alpha(e)$	0.099 ± 0.005
Γ_{be}	0.107 ± 0.005
Γ_{bce}	0.0945 ± 0.0155
$\Gamma_{b\mu}$	0.103 ± 0.005
$\Gamma_{bc\mu}$	0.0945 ± 0.0155

The values of χ,Γ_{be}, Γ_{bce}, $\Gamma_{b\mu}$, and $\Gamma_{bc\mu}$ were obtained from the 1992 edition of Phys. Rev. D, Review of Particle Properties.

Factor	*Value*	*Value*	*Value*
$e\ E_T$ threshold (GeV)	5.0	5.0	5.0
$\mu\ P_T$ threshold GeV	3.0	4.0	5.0
$\Delta_{e\mu}$	248 ± 33	190 ± 25	115 ± 18
$\frac{\Delta_{ee}}{\epsilon_{TRIG}}$	445 ± 54	339 ± 66	193 ± 85
$A(b\mu)$	0.157 ± 0.001	0.122 ± 0.001	0.097 ± 0.001
$\alpha(\mu)$	0.182 ± 0.006	0.130 ± 0.008	0.126 ± 0.010
R_Δ	0.62 ± 0.21	0.51 ± 0.17	0.40 ± 0.16

The expression for the cross section is:

$$\sigma(p\bar{p}\ \rightarrow b\bar{b}\ X) = \frac{f_{bb}\Delta_{e\mu}}{\mathcal{L}(1-2\chi)^2 2(P)}$$

The factor (P) is a combination of branching fractions for b quarks decaying to leptons and acceptances for such leptons (see Section 1.4).

Inserting the appropriate factors into the expression for the cross section we find the following values of $\sigma(p\bar{p} \rightarrow b_1 b_2 X; P_{T,1} > P_{T,1}^{min}, \mid y_1 \mid < 1.0; P_{T,2} > P_{T,2}^{min}, \mid y_2 \mid < 1.0; M_{e\mu} > 5.0$ GeV):

$P_{T,1}^{min}$ (GeV)	$P_{T,2}^{min}$ (GeV)	$\sigma(p\bar{p} \rightarrow b_1 b_2 X)(\mu b)$
8.75	6.50	1.55 ± 0.71
8.75	7.50	1.74 ± 0.80
8.75	8.75	1.59 ± 0.87

Figure 25 shows the comparison between the measured cross section and the theoretical prediction. The theory points were obtained from a Monte Carlo based upon the NLO calculation of $b\bar{b}$ production by Mangano, Nason, and Ridolfi [5]. The same Monte Carlo was used to determine the ratio of the single-inclusive and double-inclusive cross sections:

$$\frac{\sigma_{the}^{b}}{\sigma_{the}^{bb}} = \frac{\sigma(p\bar{p} \rightarrow bX : P_T^b > P_{T,1}^{min}, \mid y_b \mid < 1)}{\sigma(p\bar{p} \rightarrow b_1 b_2 X : P_{T,1} > P_{T,1}^{min}, \mid y_1 \mid < 1; P_{T,2} > P_{T,2}^{min}, \mid y_2 \mid < 1; M_{e\mu} > 5)}$$

The ratios were used to convert the measured, double-inclusive cross sections to single-inclusive cross sections for comparison with previous CDF measurements. The following table gives the ratios and the results of their application. Figure 26 compares our single-inclusive results to previous CDF results as well the NDE prediction.

$P_{T,1}^{min}$ (GeV)	$P_{T,2}^{min}$ (GeV)	$\frac{\sigma_{the}^{b}}{\sigma_{the}^{bb}}$	$\sigma_{exp}^{bb} \frac{\sigma_{the}^{b}}{\sigma_{the}^{bb}}(\mu b)$
8.75	6.50	4.0	6.2 ± 2.9
8.75	7.50	5.5	9.6 ± 4.4
8.75	8.75	8.0	12.7 ± 7.0

Figure 27 shows the sign-subtracted $\Delta\phi_{e\mu}$ distribution for events pasing all the analysis cuts, where $\Delta\phi_{e\mu}$ is the angle between the electron and muon in the transverse plane.

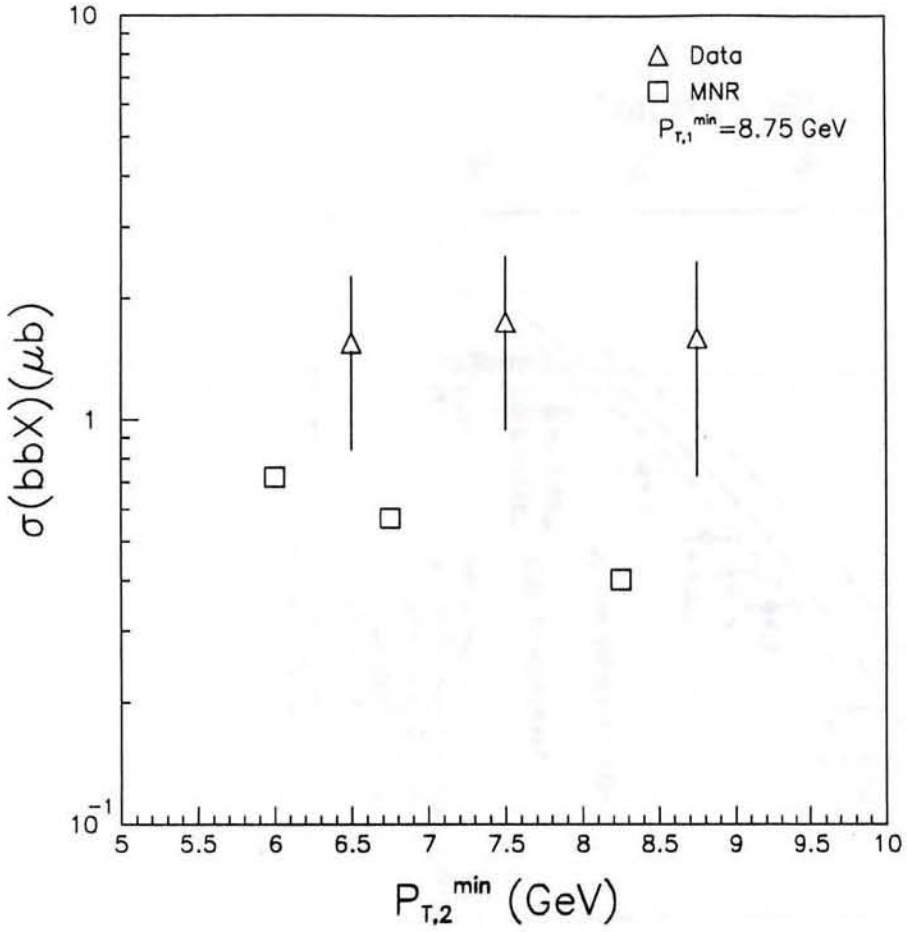

Figure 25: A comparison between the measured cross section for $p\bar{p} \rightarrow b\bar{b}$ X and the prediction from the MNR Monte Carlo.

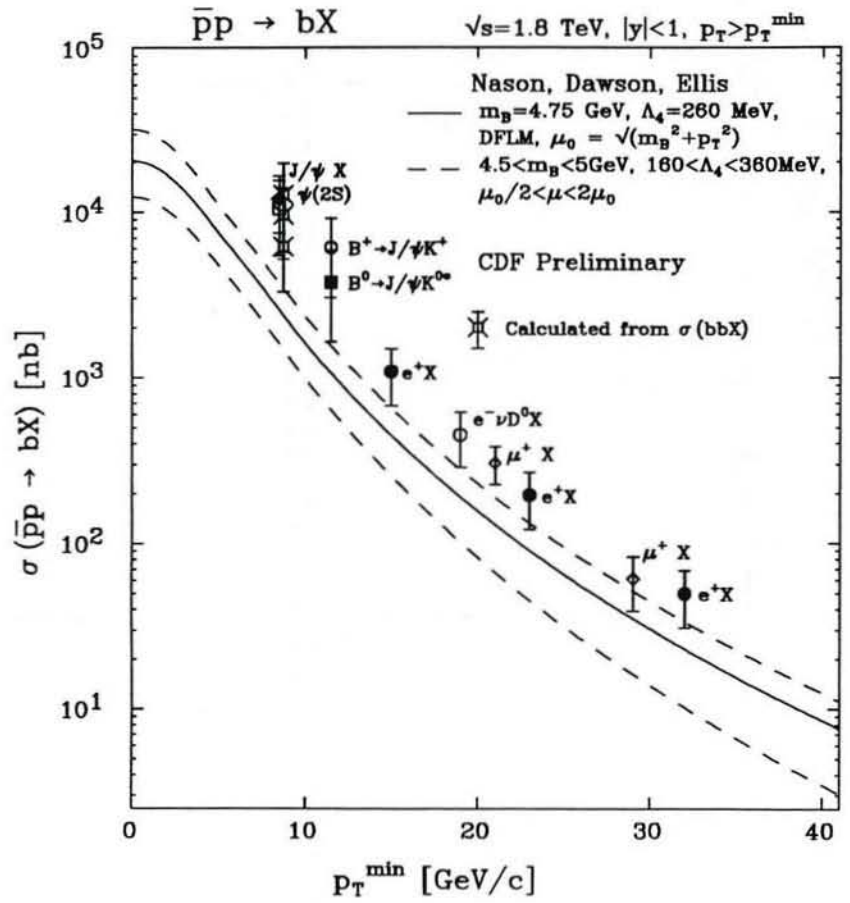
$\bar{p}p \rightarrow bX$
$\sqrt{s}$=1.8 TeV, |y|<1, $p_T > p_T^{min}$
Nason, Dawson, Ellis
m_B=4.75 GeV, Λ_4=260 MeV,
DFLM, $\mu_0 = \sqrt{(m_B^2 + p_T^2)}$
4.5<m_B<5GeV, 160<Λ_4<360MeV,
$\mu_0/2 < \mu < 2\mu_0$
CDF Preliminary
Calculated from σ (bbX)
J/ψ X
ψ(2S)
$B^+ \rightarrow J/\psi K^+$
$B^0 \rightarrow J/\psi K^{0*}$
e^+X
$e^-\nu D^0 X$
$\mu^+ X$
e^+X
$\mu^+ X$
e^+X
$\sigma(\bar{p}p \rightarrow bX)$ [nb]
p_T^{min} [GeV/c]
10^5
10^4
10^3
10^2
10^1
0
10
20
30
40

Figure 26:

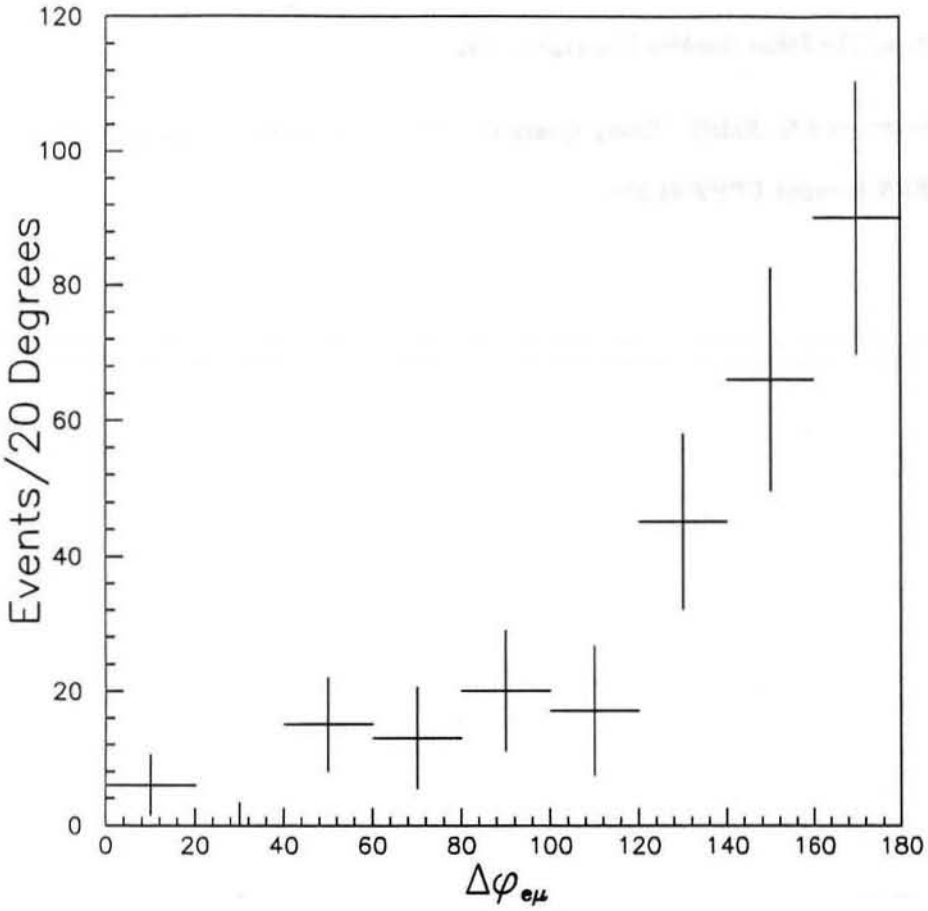

Figure 27: The sign subtracted $\Delta\phi_{e\mu}$ distribution for $e\mu$ data set.

References

[1] L. Song, *et. al.*, *Measurement of the $B^0\overline{B}^0$ Mixing Using Electron-Muon Events*, CDF1355

[2] D. Frei, *Multiple Scattering of Central Muons*, CDF1430

[3] R. E. Hughes, Dissertation, University of Pennsylvania, 1992

[4] S. Vejcik, Dissertation, The Johns Hopkins University, 1992

[5] M. Mangano, P. Nason, and G. Ridolfi "Heavy Quark Correlations in Hadron Collisions at Next-To-Leading Order", INFN Preprint UPRF-91-308